จุฬาลงกรณ์มหาวิทยาลัย

ทุนวิจัย

กองทุนรัชดาภิเษกสมโภช

รายงานผลการวิจัย

การตรึงอาร์จีดีเพปไทด์บนพื้นผิวของพอลิคาร์บอเนตที่มีไทโรซีนเพื่อเพิ่มการยึดเกาะและการเพิ่มจำนวนของเซลล์

โดย

ผู้ช่วยศาสตราจารย์ ดร. วรวีร์ โฮเว่น

ศาสตราจารย์ ดร. โยคิม โคน

นายอดิศร ผู้พัฒนพงศ์

สิงหาคม 2549

จุฬาลงกรณ์มหาวิทยาลัย

ทุนวิจัย

กองทุนรัชดาภิเษกสมโภช

รายงานผลการวิจัย

การตรึงอาร์จีดีเพปไทด์บนพื้นผิวของพอลิคาร์บอเนตที่มีไทโรซีนเพื่อเพิ่มการยึดเกาะ

และการเพิ่มจำนวนของเซลล์

โดย

ผู้ช่วยศาสตราจารย์ ดร. วรวีร์ โฮเว่น

ศาสตราจารย์ ดร. โยคิม โคน

นายอดิศร ผู้พัฒนพงศ์

สิงหาคม 2549

Acknowledgement

The authors acknowledge the financial support from Ratchadapisek Sompoj Endowment Fund. Special thanks go to Miss Supranee Buranapraditkun from Allergy and Clinical Immunology Unit, Department of Medicine, Faculty of Medicine, Chulalongkorn University for her excellent assistance and suggestions on cell culture studies. XPS analyses by Assoc. Prof. Dr. Yasuhiko Iwasaki from Tokyo Medical and Dental University, Japan is greatly appreciated.

บทคัดย่อ

ชื่อโครงการวิจัย การตรึงอาร์จีดีเพปไทด์บนพื้นผิวของพอลิคาร์บอเนตที่มีไทโรซีนเพื่อเพิ่มการยึดเกาะและการเพิ่มจำนวนของเซลล์

ชื่อผู้วิจัย วรวีร์ โฮเว่น, โยคิม โคน, อดิศร ผู้พัฒนพงศ์

เดือนและปีที่ทำวิจัยสำเร็จ พฤษภาคม 2549

งานวิจัยนี้เป็นการศึกษาการตรึงทางเคมีของเพปไทด์ที่มีลำดับกรดแอมิโนอาร์จีดี (อาร์จีดี อาร์จีดีเอสและจีอาร์จีดีเอส) บนพื้นผิวของพอลิคาร์บอเนตที่มีไทโรซีน ซึ่งมีหมู่คาร์บอกซิลเป็นหมู่ข้าง, พอลิ(ดีทีอี-โค-20%ดีที)คาร์บอเนต โดยผ่านปฏิกิริยา 2 ขั้นตอน ปฏิกิริยาในขั้นแรกเกี่ยวข้องกับการกระตุ้นหมู่คาร์บอกซิลด้วยเอ็น-ไฮดรอกซีซักซินิไมด์ (เอ็นเอชเอส) ในภาวะที่มี 1-(3-ไดเมทิลแอมิโนโพรพิล)-3-เอทิลคาร์โบไดอิไมด์ ไฮโดรคลอไรด์ (อีดีซีไอ) ขั้นที่สองเป็นการติดอาร์จีดีเพปไทด์ด้วยพันธะโควาเลนต์ โดยติดตามความสำเร็จของการตรึงเพปไทด์ด้วยวิธีนินไฮดรินและเทคนิคเอ็กซ์เรย์โฟโตอิเล็กตรอนสเปกโทรสโกปี (เอ็กพีเอส) จากการใช้สารละลายเฮกซะเมทิลีนไดแอมีนเป็นสารมาตรฐานพบว่าสามารถคำนวณความหนาแน่นของหมู่แอมิโนได้ประมาณ 8.07×10^{-8} 6.51×10^{-8} และ 5.13×10^{-8} โมล/ตารางเซนติเมตร สำหรับการตรึงด้วยอาร์จีดี อาร์จีดีเอส และจีอาร์จีดีเอส ตามลำดับ และจากการวิเคราะห์พื้นผิวของพอลิ(ดีทีอี-โค-20%ดีที)คาร์บอเนตที่ตรึงด้วยอาร์จีดีเพปไทด์หลังจากติดฉลากด้วยเฮปทาฟลูออโรบิวทิริลคลอไรด์ด้วยเทคนิคเอ็กพีเอสพบว่าได้เปอร์เซ็นต์การแทนที่ของ อาร์จีดีเอส และจีอาร์จีดีเอส เป็น 75 และ 30 เปอร์เซ็นต์ตามลำดับ จากผลจากการศึกษาความเข้ากันได้กับเซลล์ในห้องปฏิบัติการพบว่าจีอาร์จีดีเอสมีประสิทธิภาพสูงสุดในการเพิ่มการยึดเกาะและการแบ่งตัวของเซลล์ไฟโบรบลาสต์ (บี95) เมื่อเปรียบเทียบกับพอลิสไตรีนที่ใช้เลี้ยงเซลล์ (ทีซีพีเอส) ค่าสัดส่วนการยึดเกาะและการแบ่งตัวของเซลล์เพิ่มขึ้นจาก 92 และ 100 เปอร์เซ็นต์ เป็น 117 และ 129 เปอร์เซ็นต์ ตามลำดับ หลังการตรึงด้วยจีอาร์จีดีเอส จากผลการทดลองแสดงให้เห็นว่าหมู่ไกลซีนที่เพิ่มขึ้นมาทำให้เพปไทด์มีอิสระในการเคลื่อนที่ส่งผลให้ส่วนที่เป็นลำดับอาร์จีดีสามารถแสดงการตอบสนองต่อเซลล์อย่างจำเพาะเจาะจงได้อย่างมีประสิทธิภาพ

Abstract

Project Title Immobilization of RGD Peptides on Surface of Tyrosine-Derived Polycarbonate to Enhance Cell Adhesion and Proliferation

Name of the Investigators Voravee P. Hoven, Joachim Kohn, Adisorn Poopattanapong

Year 2006

This research has focused on chemical immobilization of RGD-containing peptides (RGD, RGDS, GRGDS) on the surface of tyrosine-derived polycarbonates having carboxyl pendant groups, poly(DTE-*co*-20%DT carbonate) through a two-step reaction. The first step involved an activation of carboxyl groups by *N*-hydroxysuccinimide (NHS) in the presence of 1-(3-dimethylaminopropyl)-3-ethylcarbodiimide hydrochloride (EDCI). The second step was a covalent attachment of RGD-containing peptides. The success of peptide immobilization was determined by ninhydrin method and x-ray photoelectron spectroscopy (XPS). Using hexamethylenediamine as a standard, the grafting density of ~ 8.07×10^{-8}, 6.51×10^{-8}, and 5.13×10^{-8} mol/cm^2 were estimated for the immobilization of RGD, RGDS, and GRGDS, respectively. According to XPS analysis of RGD-immobilized poly(DTE-*co*-20%DT carbonate) surface after labeling with heptafluorobutyryl chloride, 30 and 74% substitution were calculated for the immobilization of RGDS and GRGDS, respectively. Results from *in vitro* cell studies demonstrated that among all studied RGD-containing peptides, GRGDS can best enhance fibroblast (B95) adhesion and proliferation on the polymer surface. Taking 100% of TCPS as a positive control, cell adhesion ratio and proliferation ratio were elevated from 92 and 100% of the virgin polymer to 117 and 129% respectively, after GRGDS immobilization. Evidently, the extra glycine spacer introduces the flexibility to the peptide and thus allows the RGD part to effectively mediate its specific response to the cells.

Table of Contents

Page

ACKNOWLEDGEMENT..... ii
ABSTRACT IN THAI..... iii
ABSTRACT IN ENGLISH.....iv
LIST OF FIGURES.....viii
LIST OF TABLES.....xii

CHAPTER I INTRODUCTION.....1
1.1 Statement of Problem.....1
1.2 Objectives.....1
1.3 Scope of Investigation.....2

CHAPTER II THEORY AND LITERATURE REVIEW.....3
2.1 Historic Overview of Tyrosine-derived Polycarbonates.....3
2.2 The Cell-adhesive Peptide Arg-Gly-Asp (RGD).....9
2.3 Surface Modification of Biomaterial by Immobilization of Biomolecules.....13
2.3.1 Crosslinking and Conjugation Reactions.....14
2.3.2 Chemical Reactivity of Proteins.....15
2.3.3 Nucleophilic Substitution and Addition Reactions.....19
2.3.4 Immobilization of RGD Peptides on Polymers.....19
2.4 Analysis of RGD-modified Polymers.....25
2.5 Cell Surface and Cell Adhesion.....26

CHAPTER III EXPERIMENTAL.....30
3.1 Materials.....30
3.2 Equipments.....31
3.2.1 Nuclear Magnetic Resonance (NMR).....31
3.2.2 Contact Angle Measurements.....31

Page

3.2.3 X-ray Photoelectron Spectroscopy (XPS).....31
3.2.4 Attenuated Total Reflectance-Fourier Transform Infrared Spectroscopy (ATR-FTIR)……...……32
3.2.5 UV-Spectroscopy.....32
3.2.6 Hemocytometer.....32
3.2.7 Statistical Analysis.....33
3.3 Methods….....33
3.3.1 Activation of Poly(DTE-*co*-20%DT carbonate) with *N*-hydroxysuccinimide under Homogeneous Condition.....33
3.3.2 Preparation of Poly(DTE-*co*-20%DT carbonate) Films.....33
3.3.3 Activation of Poly(DTE-*co*-20%DT carbonate) with *N*-hydroxysuccinimide under Heterogeneous Condition.....34
3.3.4 Synthesis of L-3,5-Dibromotyrosine.....34
3.3.5 Reaction of Activated Poly(DTE-*co*-20%DT carbonate) Film with L-3,5-Dibromotyrosine.....34
3.3.6 Reaction of Activated Poly(DTE-*co*-20%DT carbonate) Film with RGD-containing Peptide..... 35
3.3.7 Labeling of Immobilized RGD-containing Peptide by Heptafluorobutyryl chloride.....35
3.3.8 Determination of the Amino Groups on Poly(DTE-*co*-20%DT carbonate) surface after RGD Immobilization.....35
3.3.9 Cell study.....36

CHAPTER IV RESULTS AND DISCUSSION.....……37

Page

4.1 Activation of Poly(DTE-*co*-20%DT carbonate) with *N*-hydroxysuccinimide under Homogeneous Condition.....38
4.2 Activation of Poly(DTE-*co*-20%DT carbonate) with *N*-hydroxysuccinimide under Heterogeneous Condition.....40
4.2.1 Effect of Solvent.....40
4.2.2 Effect of NHS/EDCI Concentration.....43
4.2.3 Effect of Reaction Time.....44
4.3 Reaction of Activation of Poly(DTE-*co*-20%DT carbonate) Film with L-3,5-Dibromotyrosine.....45
4.3.1 Synthesis of L-3,5-Dibromotyrosine.....46
4.3.2 Attachment of L-3,5-Dibromotyrosine on the Surface of Activated Poly(DTE-*co*-20%DT carbonate) Film.....47
4.4 Attachment of RGD-containing Peptides on the Surface of Activated Poly(DT-*co*-20%DT carbonate) Film.....48
4.4.1 Effect of Immobilization Time.....50
4.4.2 Effect of RGD-containing Peptide Concentration.....50
4.4.3 Effect of RGD-containing Peptide.....51
4.5 Cell Study.....54

CHAPTER V CONCLUSION AND SUGGESTION.....56
REFERENCES.....58
APPENDICES.....62
APPENDIX A.....63
APPENDIX B.....66
APPENDIX C.....75

LIST OF FIGURES

Figure Page

2.1 Chemical structures of (A) tyrosine-derived polycarbonates, (B) tyrosine-derived polyarylates....4
2.2 Chemical structures of Bisphenol A and tyrosine dipeptide....5
Chemical structure of desaminotyrosyl-tyrosine alkyl esters, abbreviated 'DTR' 6
2.4 Schematic summary of the mechanism of degradation of tyrosine-derived polycarbonates....7
2.5 Chemical structure of RGD....10
2.6 Schematic drawing of the general structure of integrin. Two types of integrins are shown, one with an α subunit which is proteolytically processed into two disulfide-linked fragments at a cleavage site (shown as a gap in the structure on the left). Other integrins have subunits that are not processed....11
2.7 Integrin family....12
2.8 Reactive groups of amino acid side chains. Functional groups A to F are the six most reactive entities. G and H are less reactive. (A) amino groups of N-terminal amino acids and -amino groups of lysines; (B) carboxyl groups of aspartic, glutamic acids and C-terminal amino acids; (C) thiol group of cysteine; (D) thioether of methionine; (E) imidazolyl group of histidine; (F) guanidinyl group of arginine; (G) phenolic group of tyrosine; and (H) indolyl group of tryptophan....17

LIST OF FIGURES (Continued)

Figure Page

2.9 RGD peptides react via the *N*-terminus with different groups on polymers: (A) carboxyl groups, preactivated with a carbodiimide and NHS to generate an active ester, (B) amino groups, preactivated with DSC, (C) hydroxyl groups, preactivated as tresylate, (D) hydroxyl groups, preactivated as *p*-nitrophenyl carbonate.....21

2.10 Chemoselective ligation of selected pairs of functional groups. (A) thiol and bromoacetyl-RGD. (B) aldehyde and aminooxy-RGD. (C) acrylate and thiol-RGD. (D) maleinimide and thiol-RGD.....23

2.11 Schematic representation of the modification route. Surface Ti: water-vapor plasma-pretreated titanium; Surface A: poly(3-aminopropyl) siloxane pendant surface; Surface M: maleimide-modified surfaces with different alkyl chains; Surface P: peptide- or L-cysteine-modified surfaces; H-SR: L-cysteine, RGDC, GRGDSPC.....24

4.1 Mechanism of an activation of surface carboxyl group followed by a coupling reaction with RGD-containing peptide.....37

4.2 ^{1}H NMR spectra of (a) poly(DTE-*co*-20%DT carbonate) and poly(DTE-*co*-20%DT carbonate) after reacted with *N*-hydroxysuccinimide in (b) tetrahydrofuran and (c) 10% (v/v) methanol/methylene chloride.....39

4.3 Water contact angle of poly(DTE-*co*-20%DT carbonate) film after the reaction with aqueous solution of 0.1 M NHS/EDCI: advancing (○) and receding (●) …….....41

4.4 ATR-FTIR spectra of poly(DTE-*co*-20%DT carbonate) and activated poly(DTE-*co*-20%DT carbonate) films.....42

LIST OF FIGURES (Continued)

Figure Page

4.5 ^{1}H NMR spectra of poly(DTE-*co*-20%DT carbonate) film after the reaction with 0.1 M NHS/EDCI in (a) water, (b) 20% ethanol/water, (c) 50% ethanol/water and (d) ethanol for 2 h....43

4.6 %Yield of activation of poly(DTE-*co*-20%DT carbonate) film after reaction with NHS/EDCI solution in ethanol for 2 h as a function of NHS/EDCI concentration....44

4.7 % Yield of activation of poly(DTE-*co*-20%DT carbonate) film after reaction with a varied concentration of NHS/EDCI solution in ethanol as a function of reaction time**:** 0.1 M (●) and 0.05 M (○).....45

4.8 ^{1}H NMR spectrum of L-3,5-dibromotyrosine....46

4.9 Chemical structures of RGD, RGDS and GRGDS....49

4.10 Calibration curve of UV absorbance as a function of 1,6-hexanediamine concentration using ninhydrin method....49

4.11 Amino concentration per surface area of immobilized RGD on poly(DTE-*co*-20%DT carbonate) surface as a function of immobilization time....50

4.12 Amino concentration per surface area of immobilized RGD on poly(DTE-*co*-20%DT carbonate) surface as a function of peptide concentration....51

4.13 Amino concentration per surface area of immobilized RGD-containing peptides on poly(DTE-*co*-20%DT carbonate) surface using the peptide concentration of 0.05 M and immobilization time of 24h....52

4.14 *In vitro* cell adhesion ratio (CAR) of fibroblasts on polymer substrates.....55

4.15 *In vitro* cell proliferation ratio (CPR) of fibroblasts on polymer substrates....55

LIST OF FIGURES (Continued)

Figure Page

A-1 The ^{1}H-NMR (400 MHz $CDCl_3$) of poly(DTE-*co*-20%DT carbonate) film.....64

A-2 The ^{1}H-NMR (400 MHz $CDCl_3$) of activated poly(DTE-*co*-20%DT carbonate) film.....64

A-3 The ^{1}H-NMR (400 MHz DCl) of L-3,5-dibromotyrosine.....65

B-1 Calibration curve of UV-absorbance as a function of 1,6-hexanediamine concentration analyzed by ninhydrin method.....69

LIST OF TABLES

Table Page

2.1 Physico-mechanical properties of tyrosine-derived polycarbonates.....8
2.2 Cell attachment and proliferation on surfaces of tyrosine-derived polycarbonates.....9
2.3 Nature and properties of physical adsorption and chemical binding.....14
2.4 Chemical modification of amino acid side chains.....17
2.5 pKa of some reactive groups in amino acids and model peptides.....18
4.1 Atomic composition of controlled poly(DTE-*co*-20%DT carbonate) film and NHS-activated poly(DTE-*co*-20%DT carbonate) film after L-3,5-dibromotyrosine attachment.....48
4.2 Atomic composition RGD-immobilized poly(DTE-*co*-20%DT carbonate) film after labeling with heptafluorobutyryl chloride.....54
B-1 Water contact angle of activated poly(DTE-*co*-20%DT carbonate) films after reaction with *N*-hydroxysuccinimide in water as a function of reaction time.....67
B-2 %Yield of activation of poly(DTE-*co*-20%DT carbonate) with *N*-hydroxysuccinimide as a function of coupling agent concentration.....67
B-3 %Yield of activation of poly(DTE-*co*-20%DT carbonate) with *N*-hydroxysuccinimide as a function of reaction time.....68
B-4 UV-absorbance at λ = 538 nm of standard 1,6-hexanediamine solution for generating a calibration curve.....68
B-5 Amino content of RGD-poly(DTE-*co*-20%DT carbonate) film as a function of immobilization time.....70
B-6 Amino-content of RGD-poly(DTE-*co*-20%DT carbonate) film as a function of RGD concentration.....71

LIST OF TABLES (Continued)

Tables Page

B-7 Amino contents of RGDS-poly(DTE-*co*-20%DT carbonate) and GRGDS-poly(DTE-*co*-20%DT carbonate) using peptide concentration of 0.05 M.....72
B-8 Number of fibroblast attachment on polymer surfaces after 12 h incubation.....73
B-9 Number of fibroblast proliferation on polymer surface.....74

CHAPTER I

INTRODUCTION

1.1 Statement of Problem

Nowadays a large number of synthetic polymeric materials with various different properties are available for medical applications. Most of the common materials have sufficient mechanical stability and elasticity as well as desired stability towards degradation, and are non-toxic. One important remaining problem is inadequate interaction between polymer and cells, leading to *in vivo* foreign body reactions, such as inflammation, infections, aseptic loosening, local tissue waste, and implant encapsulation as well as thrombosis and embolization. Approaches to improve biomaterials include reduction of unspecific protein adsorption, known as non-fouling properties, enhancement of adsorption of specific proteins, and material modification by immobilization of cell recognition motives to obtain controlled interaction between cells and synthetic substrates.

Polymeric biomaterials possessing specific cellular responses have become increasingly important in some biomedical applications of which biocompatibility is critically required, for example, prostheses, implants and tissue engineering matrices. Considerable success has been continuously reported on the material modification by immobilization of cell recognition motives to obtain desirable cellular responses. The RGD (R: arginine; G: glycine; D: aspartic acid) sequence is by far the most effective and most often employed cell recognition motives for stimulating cell adhesion on synthetic surfaces. Since its discovery in 1984 by Pierschbacher and Ruoslahti, RGD peptides have gained their reputation of being able not only to trigger cell adhesion effectively, but also to address selectively certain cell lines and elicit specific cellular responses. This tripeptide sequence is uniquely specific to integrin, a cell adhesion receptor at the cell membrane which is responsible for mediating cell adhesion and proliferation.

Tyrosine-derived polycarbonates having carboxyl pendant groups, poly (desaminotyrosyl-tyrosine ethyl ester-co-desaminotyrosyl-tyrosine carbonate) (poly(DTE-*co*-DT carbonate)), have been recently introduced as a new series of biodegradable polymer that can be potentially used for biomedical applications. The carboxyl groups can serve as versatile precursors for a wide range of chemical modification including an attachment with bioactive molecules including proteins and peptides.

This research aims to improve cellular responses of poly(DTE-*co*-DT carbonate by RGD attachment. An amide linkage is formed by reacting an activated carboxyl group with the nucleophilic *N*-terminus of the RGD peptides. Carboxyl groups can be activated by *N*-hydroxysuccinimide/1-ethyl-3-(3-dimethylaminopropyl) -carbodiimide (NHS/EDCI). *In vitro* adhesion and proliferation of fibroblasts are conducted in order to determine cellular responses of RGD-modified polycarbonates.

1.2 Objectives

1. To immobilize RGD-containing peptides on poly(DTE-*co*-DT carbonate) surfaces
2. To determine *in vitro* cell adhesion and proliferation of poly(DTE-*co*-20%DT carbonate) surfaces after immobilized with RGD-containing peptides

1.3 Scope of Investigation

The stepwise investigation was carried out as follows.

1. Literature survey for related research work.
2. To activate carboxyl groups of poly(DTE-*co*-DT carbonate) with *N*-hydroxysuccinimide under homogeneous condition
3. To activate carboxyl groups of poly(DTE-*co*-DT carbonate) with *N*-hydroxysuccinimide under heterogeneous condition
4. To immobilize RGD-containing peptides on poly(DTE-*co*-DT carbonate) surface
5. To determine *in vitro* cell adhesion and proliferation

CHAPTER II

THEORY AND LITERATURE REVIEW

2.1 Historic Overview of Tyrosine-derived Polycarbonates [1]

Over the last 25 years, significant efforts have been devoted to the development of polymeric biomaterials. Historically, the vast majority of these efforts were focused on identifying 'off the shelf' polymers that were biologically inert and stable under physiological conditions. These materials were used as permanent prosthesis such as bone and joint replacements, dental devices and cosmetic implants. However, the emerging fields of tissue engineering and the need for advanced drug and gene delivery systems have resulted in an increasing need for resorbable and/or degradable polymers.

The main driving forces for the development of new, resorbable and/or degradable biomaterials are (i) the need of the pharmaceutical industry to develop advanced drug delivery systems for the many new peptide and protein drugs that will become available through biotechnology and genomics, (ii) the need of the medical device industry to develop degradable implants (scaffolds) for tissue regeneration and tissue engineering applications, and (iii) the need to improve the biocompatibility of biosensors and implantable medical devices. This last application calls for new materials with surfaces that prevent scarring and/or protein adsorption at the implant/tissue interface.

Pseudo-poly(amino acid)s have been extensively studied and have found practical, biomedical applications. They were first described in 1984 [2]. Naturally occurring amino acids are linked by non-amide bonds, such as ester, iminocarbonate and carbonate bonds. The resulting polymers contain the same monomeric building blocks as conventional poly(amino acid)s, but do not have a peptide-like backbone structure. For example, tyrosine-derived polycarbonates and tyrosine-derived polyarylates are shown below.

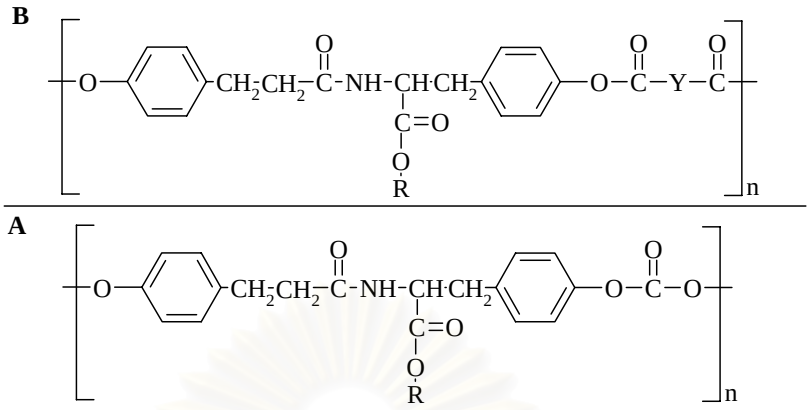

Figure 2.1 Chemical structures of (A) tyrosine-derived polycarbonates, (B) tyrosine-derived polyarylates.

Diphenols, such as Bisphenol A, are frequently used in industry, since their aromatic backbone structures can significantly increase the stiffness and mechanical strength of polymers. However, Bis-phenol A and other industrially used diphenols are cytotoxic and can therefore not be used as monomers in degradable biomaterials. There was a significant need for a non-cytotoxic, diphenolic monomer that could be used as a building block in the design of degradable implant materials. This need was addressed by the development of several tyrosine-based monomers. Tyrosine is the only major, natural nutrient containing an aromatic hydroxyl group. In view of the non-processibility of conventional poly-(L-tyrosine), which cannot be used as an engineering plastic, the development of a tyrosine-based pseudo-poly(amino acid) was envisioned. In this context, derivatives of tyrosine dipeptide can be regarded as diphenols and may be employed as replacements for the industrially used diphenols in the design of medical implant materials (Figure 2.2). This approach led, for the first time, to tyrosine-derived polymers with favorable engineering properties.

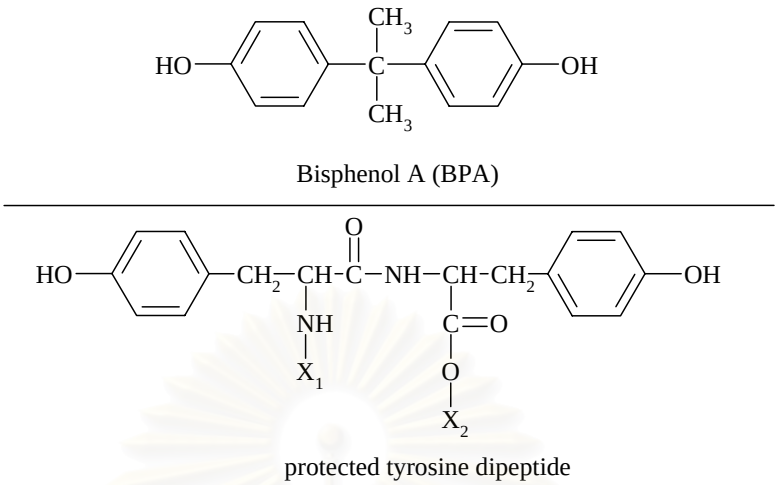

Figure 2.2 Chemical structures of tyrosine dipeptide and Bisphenol A.

In the dipeptide structure, the amino terminal group and the carboxylic acid terminal group are shown with appropriate chemical protecting groups attached (X_1 and X_2). The nature of these protecting groups affects the chemical synthesis of the polymer as well as the final physicomechanical properties of the resulting polymer. The challenge of the early studies was to identify suitable protecting groups that will lead to non-toxic, fully degradable polymers with good engineering properties. The combination of these different properties within one single design proved to be a difficult task and early investigations did not lead to readily processable materials. Later, it was recognized that the number of inter-chain hydrogen bonding sites per monomer unit had to be minimized. These studies led to the replacement of one tyrosine molecule by desaminotyrosine [3-(4'-hydroxyphenyl)propionic acid] and the identification of desaminotyrosyl-tyrosine alkyl esters (Figure 2.3) as fully biocompatible replacements for Bisphenol A and other industrial diphenols in a wide range of polymers. Monomer synthesis from 3-(4'-hydroxy phenyl) propionic acid and tyrosine alkyl esters was accomplished by carbodiimide-mediated coupling reactions, following known procedures of peptide synthesis [3], giving typical yields of 70%. Monomers carrying an ethyl, butyl, hexyl, or octyl ester pendent chain have been investigated extensively. The carboxylic acid terminal group is protected by an alkyl ester which can be regarded as a pendent chain after polymerization. The structure of the alkyl esters is indicated by the following nomenclature convention:

DTE, de-saminotyrosyl-tyrosine ethyl ester; DTB, desaminotyrosyl-tyrosine butyl ester; DTH, desaminotyrosyl-tyrosine hexyl ester; DTO, desaminotyrosyl-tyrosine octyl ester.

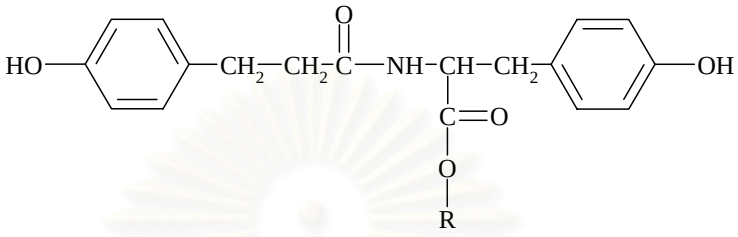

Figure 2.3 Chemical structure of desaminotyrosyl-tyrosine alkyl esters, abbreviated 'DTR'.

Tyrosine-derived polycarbonates are a group of 'homologous' carbonate–amide copolymers differing only in the length of their respective alkyl ester pendent chains. The diphenolic monomers were polymerized using either phosgene or the more easily handled bis(chloromethyl) carbonate tri-phosgene. Polymers with weight-average molecular weights (M_w) of up to 400,000 were obtained [3], although for practical applications, M_w values around 100,000 are usually preferred. Polymer properties, such as glass transition temperature, surface free energy, and mechanical properties, can be easily controlled by varying the length of the alkyl ester pendent chain. Surprisingly, the degradation rate is not a sensitive function of the length of the alkyl ester pendent chain, therefore all poly(DTR carbonate)s can be easily handled under ambient conditions and degrade only slowly under physiological conditions. *In vivo* studies confirmed the absence of enzymatic involvement in the degradation process

Recently, the degradation mechanism was studied in detail by Tangpasuthadol et al. [4,5] utilizing a series of small model compounds that mimic the repeat unit of the polymer, followed by a thorough 3-year degradation study. These results indicated that the backbone carbonate bond is hydrolyzed at a faster rate than the pendent chain ester bond. Only under very acidic conditions (pH $\leq$ 3) did the acid catalyzed hydrolysis of the ester bond become a dominant factor and pendent chain ester

hydrolysis outpaced the rate of hydrolysis of the backbone carbonate bonds. Increasing the length of the pendent chain from ethyl to octyl reduced the rate of hydrolysis of both the ester and carbonate bonds, possibly by hindering the access of water molecules to these bonds. The mechanism of polycarbonate degradation is shown schematically in Figure 2.4. According to this mechanism, the final degradation products *in vitro* are desaminotyrosyl-tyrosine and the alcohol used to protect the carboxylic acid group. *In vivo*, it is reasonable to expect the enzymatic degradation of desaminotyrosyl-tyrosine to desaminotyrosine and L-tyrosine.

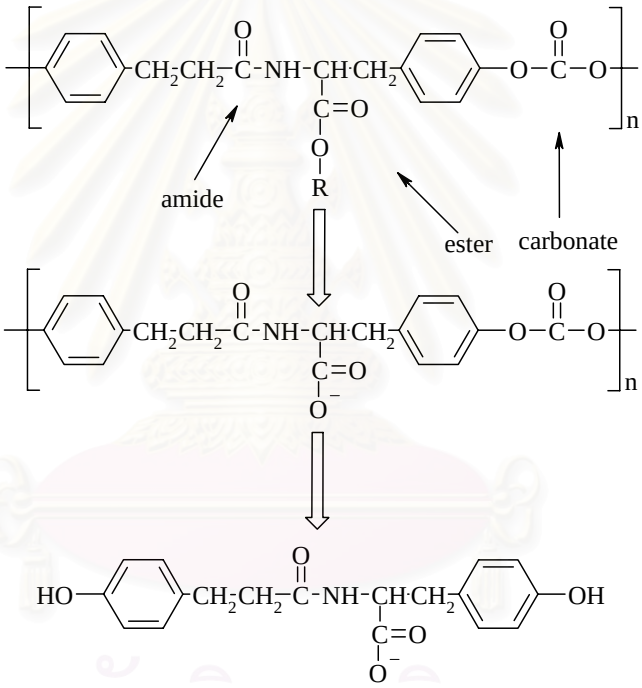

Figure 2.4 Schematic summary of the mechanism of degradation of tyrosine-derived polycarbonates.

The physicomechanical properties and potential applications of tyrosine-derived polycarbonates were studied by Ertel and Kohn. [6] Briefly, the polycarbonates are amorphous polymers. Because of their high hydrophobicity, they do not swell in aqueous media or during the degradation process. Their equilibrium water content is about 2 to 3% and remains below 5% even at advanced stages of degradation. Glass transition temperatures (T_g) range from 52 to 93 ^oC and

decomposition temperatures exceed 290 ^{o}C, providing a wide temperature window for thermal processing. Thorough evaluations of enthalpy relaxation kinetics determined that storage of polycarbonates at a temperature of T_g -15 ^{o}C for only a few hours is sufficient to bring the physical aging process to completion. Even in an unoriented stage (thin solvent cast or compression molded films), tyrosine-derived polycarbonates are characterized by their high mechanical strength (50–70 MPa) and stiffness (1–2 GPa). These values can be further increased by processing conditions that induce molecular orientation.

Table 2.1 Physico-mechanical properties of tyrosine-derived polycarbonates

Polycarbonate derived from	Molecular weight (weight average)	Glass transition temp. (^{0}C)	Decomposition temp. (^{0}C)	Water contact angle (deg)
DTE	176,000	81	290	73
DTB	120,000	66	290	77
DTH	350,000	58	320	86
DTO	450,000	53	300	90

The amino acid L-tyrosine was shown to be a versatile building block for biodegradable and biocompatible polymers. The incorporation of derivatives of tyrosine dipeptide, such as the desaminotyrosyl-tyrosine alkyl esters (DTR), into the backbone of different polymer systems results in versatile polymers with interesting properties. Contrary to most conventional poly(amino acid)s, tyrosine-derived pseudo-poly(amino acid)s exhibit excellent engineering properties and polymer systems can be designed whose members show exceptional strength (polycarbonates). In particular, the tyrosine-derived polycarbonate, poly(DTE carbonate), has been shown to have a high degree of tissue compatibility.

Table 2.2 Cell attachment and proliferation on surfaces of tyrosine-derived polycarbonates [6]

Polymer	1 day attachment (x100 cells cm^{-2})	5 day attachment (x100 cells cm^{-2})
Results for fibroblasts		
poly(DTE carbonate)	46±13	596±100
poly(DTB carbonate)	56±17	410±79
poly(DTH carbonate)	32±10	268±46
Glass (as a control surface)	50±16	555±91
Results for osteoblasts		
poly(DTE carbonate)	34±15	318±93
Glass (as a control surface)	59±22	739±83

While in the past the vast majority of all commercial research involving degradable polymers was limited to the use of poly(lactic acid), poly(glycolic acid) or copolymers thereof, it is obvious that, in the future, a wider range of new materials will be needed. Tyrosine-derived pseudo-poly(amino acid)s represent one of many new ‘second generation biomaterials’ that will enter into clinical use over the next decade.

2.2 The Cell-adhesive Peptide Arg-Gly-Asp (RGD)

In the early 80s, Pierschbacher discovered that the cell attachment activity could be mimicked by short, immobilized, synthetic peptides containing a short three amino acid sequence, arginine-glycine-aspartic acid (RGD) [7].

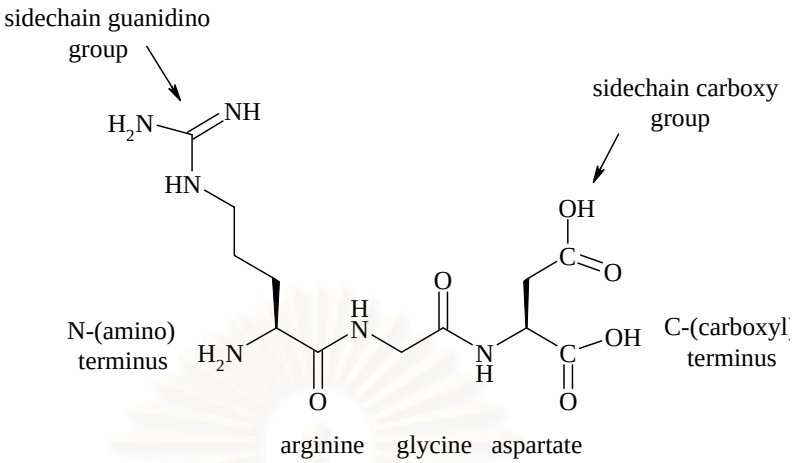

Figure 2.5 Chemical structure of RGD.

The recognition site for many of the integrins that bind to extracellular matrix and platelet adhesion proteins is the tripeptide RGD [8]. The role of the RGD sequence as the recognition site was demonstrated by making progressively smaller fragments of fibronectin and by assaying for the cell attachment-promoting activity in the fragments and in synthetic peptides reproducing the amino acid sequences of such fragments. When coated onto a surface, the fragments and synthetic peptides containing the RGD sequence promote cell attachment, whereas in solution they inhibit the attachment of cells to a surface coated with fibronectin or the peptides themselves. Changes in the peptides as small as the exchange of alanine for the glycine or glutamic acid for the aspartic acid, which constitute the addition of a single methyl or methylene group to the RGD tripeptide, or the replacement of the arginine with a lysine residue, eliminate these activities of the peptides. Conformation of the amino acids is also important; a peptide in which the aspartic acid is in the D-form is inactive. The RGD sequence is also the cell recognition site of a surprising number of other extracellular matrix (ECM) and platelet adhesion proteins. In addition to fibronectin, these include vitronectin, collagens, fibrinogen, von Willebrand factor, osteopontin, bone sialoprotein I, thrombospondin, tenascin, laminin, and entactin.

Integrins are a family of membrane glycoproteins consisting of two subunits, α and β. The structural models for the various integrins are depicted in Figure 2.6. The α subunits are homologous to one another but not to the β subunits, which form

their own homologous group. Both integrin subunits have a large extracellular domain, a trans-membrane segment, and a cytoplasmic tail. The α and β subunits are noncovalently bound to one another, and this association is promoted by divalent cations.

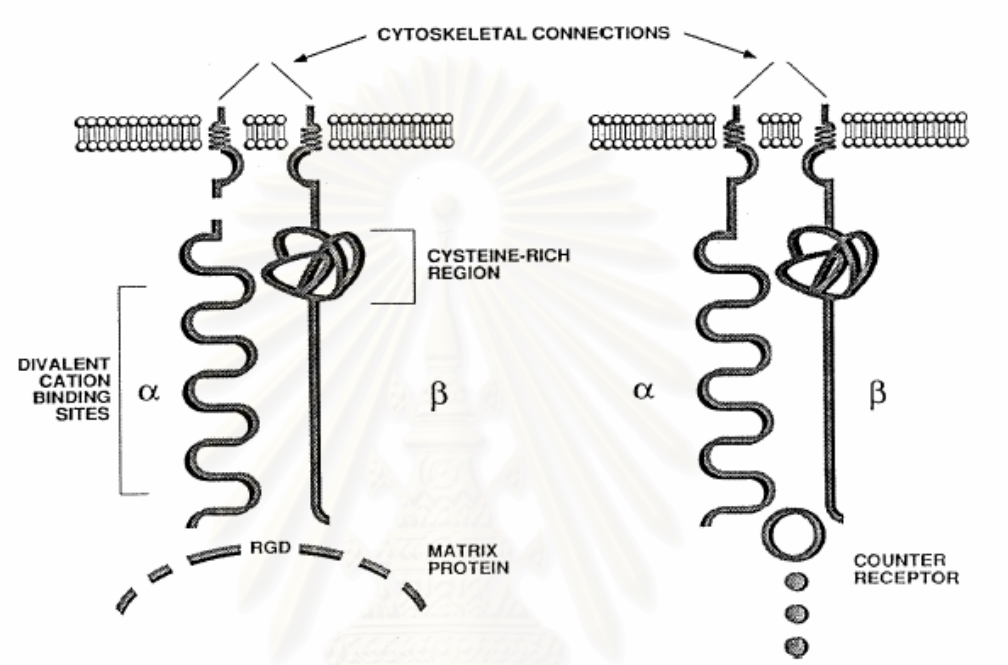

Figure 2.6 Schematic drawing of the general structure of integrin [9]. Two types of integrins are shown, one with an α subunit which is proteolytically processed into two disulfide-linked fragments at a cleavage site (shown as a gap in the structure on the left). Other integrins have subunits that are not processed.

Figure 2.7 lists the commonly accepted ligands for many integrins. The known subunits, the subunit combinations that form the known integrins, and the known ligands for these integrins are shown. Also shown is the RGD specificity of those integrins that bind to this sequence. FN, fibronectin; Fn alt., fibronectin alternatively spliced domain; LM, laminin; VN, vitronectin; Coll, collagen; vWF, von Willebrand factor; FB, fibrinogen; OP, osteopontin; BSP 1, bone sialoprotein 1; ICAM-1, ICAM-2, intercellular adhesion molecules; FX, factor X; BM, basement membrane; C3bi, complement component C3bi.

It is clear that the specificity of ligands is quite complex, for one integrin can bind more than one ECM protein, and in addition, a single ECM protein can bind to more than one integrin. In the latter case, when the binding is RGD dependent, more than one integrin is using the same general binding region on a single ECM protein, the RGD sequence.

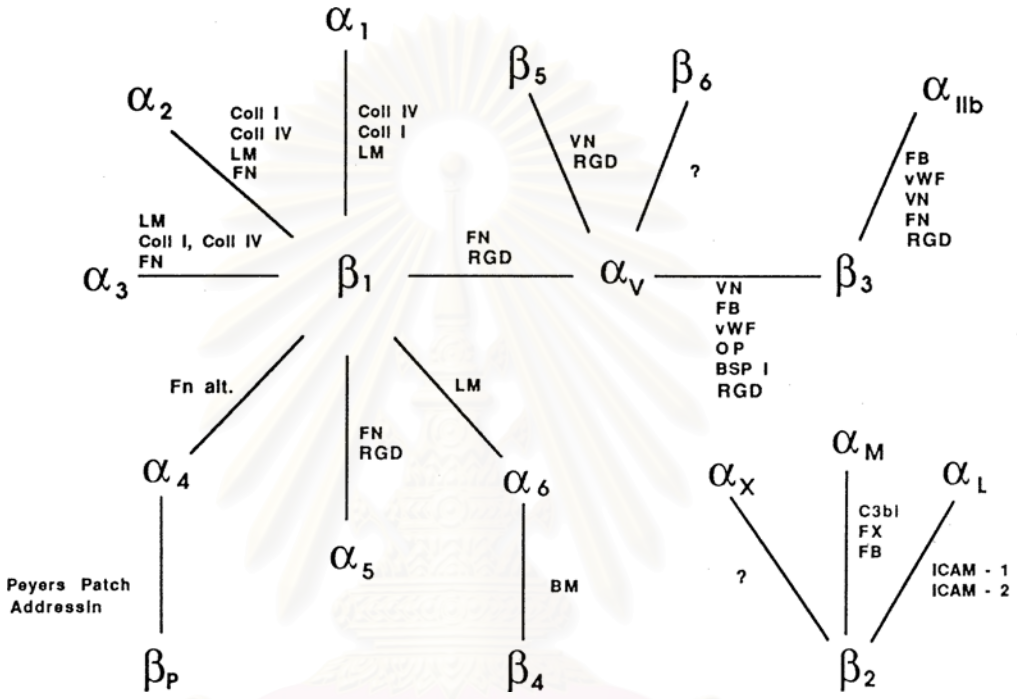

Figure 2.7 Integrin family [10].

Cell adhesion plays an important role in a variety of basic biological processes, including guiding cells into their appropriate locations in the body, providing cell anchorage, and controlling cell proliferation, differentiation, and apoptosis. Adhesion peptides have found important uses as probes for these phenomena. In addition, there are also practical applications for these peptides. Adhesive peptides can be used in two different ways: When attached to a surface, they promote cell attachment, whereas when presented in solution, they prevent attachment that would otherwise occur. Both modes of using the peptide have found applications. Surface-coated RGD peptides are being investigated for improvement of tissue compatibility of various implanted devices.

Other applications being explored include the targeting of the specific integrin ($\alpha_v\beta_3$) in osteoporosis. Osteoclasts attach to bone through this integrin (and possibly some other av integrins), and inhibiting their attachment with peptides prevents bone degradation *in vitro* and *in vivo*. Protein engineering with RGD can have applications in protein targeting and gene therapy with viruses. Advances in the application of RGD and related sequences to various purposes will depend on detailed understanding of integrin-ligand recognition. Much progress has been made recently in this field. Adhesion peptides, RGD in particular, have provided a great deal of information about cell adhesion mechanisms and are serving as a basis for the development of a new group of pharmaceuticals.

2.3 Surface Modification of Biomaterial by Immobilization of Biomolecules

A current trend to enhance biocompatibility consists of chemical modification of the biomaterial surface by the grafting of biologically active molecules such as peptides, proteins, and antibodies. This procedure offers the advantage of improving surface properties with respect to biocompatibility without adverse effect on the bulk properties of the system. Immobilization of such molecules can be achieved by a variety of different techniques that exploit either physical adsorption (through Van der Waals, hydrophobic, or electrostatic forces) or chemical binding. Both approaches have advantages and disadvantages. Physical adsorption processes are generally experimentally simple and often allow retention of the biomolecular activity. However, the adsorption is often reversible, with target molecules being removed by certain buffers or detergents or replaced by other molecules in solution. In contrast, chemical immobilization involves the covalent bonding (or complexation) of the target molecule to the solid phase. This method is experimentally more difficult and often exposes the molecule to a harsher environment. However, the resultant irreversible binding which can be produced with high levels of surface coverage makes this approach more popular, although in some cases chemical binding can alter the conformational structure and active center of the molecule, causing a reduction in activity. Some aspects of the physical adsorption and chemical binding are summarized in Table 2.3.

Table 2.3 Nature and properties of physical adsorption and chemical binding.

	Physical adsorption	**Chemical binding**
Principles	- Van der Waals forces - hydrophobic forces - electrostatic interactions	- covalent bond - complexation - coordination
Advantages	- easy to prepare under mild experimental conditions - adsorption reversible - biological activity retained	- controlled coverage - stable in physiological conditions and for multiple uses
Disadvantages	- not stable under all physiological conditions - one time use - poor reproducibility	- stringent reaction conditions - some biological activity may be lost

2.3.1 Crosslinking and Conjugation Reactions

The concept of cross-linking and conjugation originally stems from protein and peptide chemistry. Chemical cross-linking involves joining of two molecular components by a covalent bond achieved through the use of cross-linking reagents. The components may be proteins, drugs, nucleic acids, or solid substrates. The chemical cross-linkers are bifunctional reagents containing two reactive functional groups derived from classical chemical modification agents. The reagents are capable of reacting with the side chains of the amino acids of proteins. They may be classified into homobifunctional, heterobifunctional, and zero-length crosslinkers. The zero-length crosslinkers are essentially group-activating reagents which cause the formation of a covalent bond between the components without incorporation of any extrinsic atoms. The homobifunctional reagents consist of two identical functional groups and the heterobifunctional reagents contain two different types of reactive functional moieties. Model reactions for the three kinds of crosslinkers are shown below.

a) Carbodiimides are examples of zero-length crosslinkers

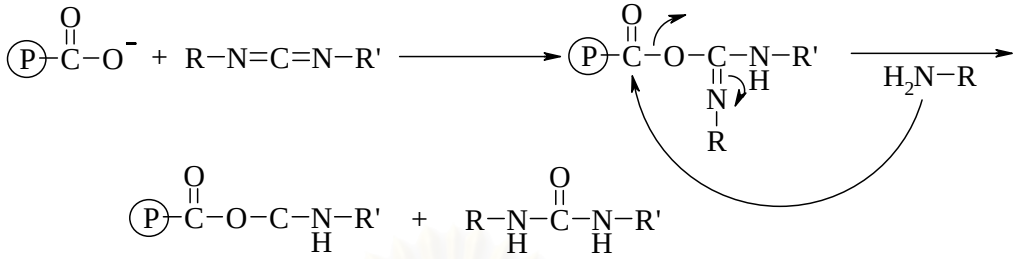

b) Reagents with bifunctional succinimidyl esters are examples of homobifunctional crosslinkers

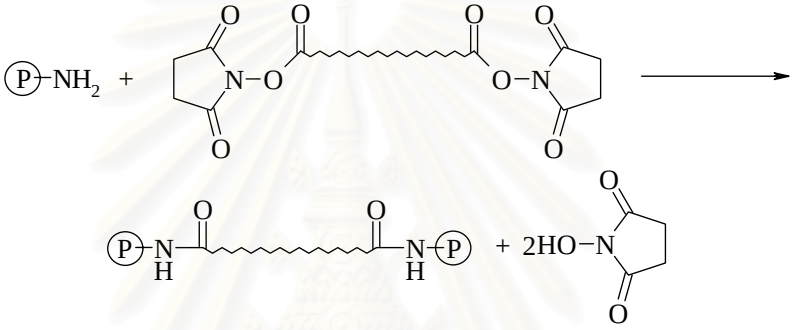

c) Reagents with succinimidyl ester- and maleimidyl groups are examples of heterobifunctional crosslinkers

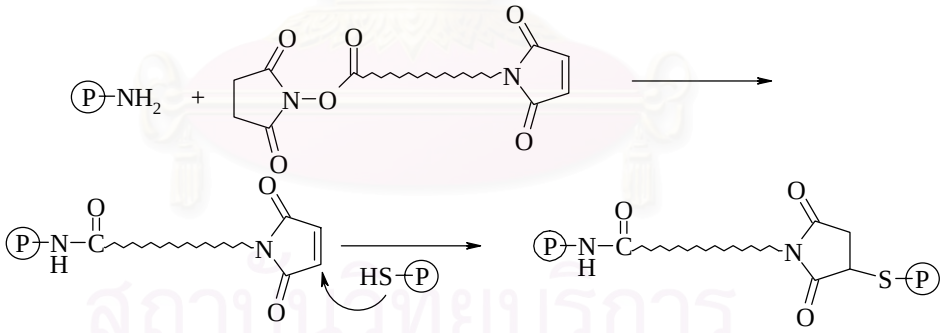

2.3.2 Chemical Reactivity of Proteins

Chemical crosslinking and conjugation of proteins and peptides depend on the reactivity of the constituents of proteins as well as the specificity of crosslinkers used. In order to preserve the biological activity of the individual protein, the reaction site on the protein must be those amino acids that are not involved in its biological functions. The biological activity loss of proteins can be caused by disturbances of their secondary and tertiary structures, their surface charges, their hydrophobic and hydrophilic properties, and their native conformations. Thus, only those amino acid

residues that are not situated at the active centers or settings critical to the integrity of the tertiary structures of proteins may be targets for chemical modification. Such amino acids must be located on the surface of the protein and are easily accessible by crosslinkers. It follows, therefore, that the identity of the reactive functional groups on the exterior of a protein is the most important factor that controls its reactivity towards crosslinking reagents. By knowing which functional groups are located at the protein - solvent interface, the protein may be modified without sacrificing its biological activity.

All proteins are composed of amino acids. There are twenty common amino acids with side chains of different sizes, shapes, charges, polarities, and chemical reactivity. These physico-chemical properties determine the precise structure and function of each individual protein. Glycine, alanine, valine, leucine, isoleucine, methionine, and proline have nonpolar aliphatic side chains while phenylalanine and tryptophan have nonpolar aromatic side groups. These hydrophobic amino acids are generally located in the interior of proteins forming the so-called hydrophobic core of many molecules. Other amino acids, arginine, aspartic acid, glutamic acid, cysteine, histidine, lysine, and tyrosine have ionizable side chains. Together with asparagine, glutamine, serine, and threonine which contain non-ionic polar groups, they are usually located on the protein surface where they can interact strongly with the aqueous environment.

The chemical reactivities of peptides and proteins depend on the side chains of their amino acid compositions as well as the free amino and carboxyl groups of the N- and C-terminal residues, respectively. Studies of chemical modification have revealed that only a few of the amino acid side chains are really reactive. Of the twenty amino acids, the alkyl side chains of the hydrophobic residues are chemically inert except the photochemical insertion. Only eight of the hydrophilic side chains are chemically active. These are the guanidinyl group of arginine, the γ - and β-carboxyl groups of glutamic and aspartic acids, respectively, the thiol group of cysteine, the imidazolyl group of histidine, the ε-amino group of lysine, the thiolether moiety of methionine, the indolyl group of tryptophan and the phenolic hydroxyl group of tyrosine (Figure 2.8). Table 2.4 summarizes the various chemical modification reactions of these active side chains. The most important reactions are alkylation and acylation. In

alkylation, an alkyl group is transferred to the nucleophilic atom, whereas in acylation, an acyl group is bonded.

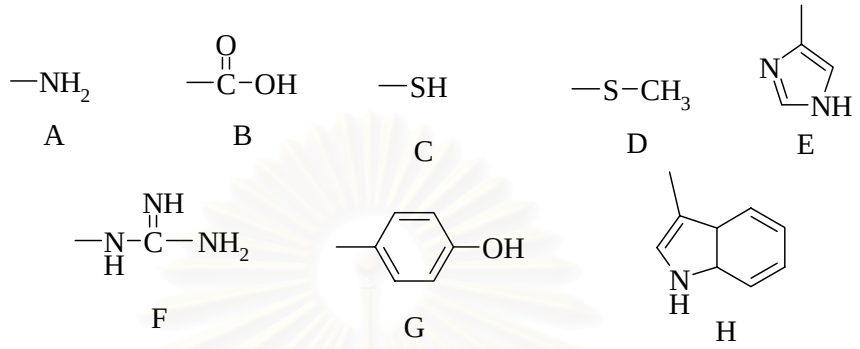

Figure 2.8 Reactive groups of amino acid side chains. Functional groups A to F are the six most reactive entities. G and H are less reactive. (A) amino groups of N-terminal amino acids and -amino groups of lysines; (B) carboxyl groups of aspartic, glutamic acids and C-terminal amino acids; (C) thiol group of cysteine; (D) thioether of methionine; (E) imidazolyl group of histidine; (F) guanidinyl group of arginine; (G) phenolic group of tyrosine; and (H) indolyl group of tryptophan.

Table 2.4 Chemical modification of amino acid side chains

Amino Acid	Side Chain	Alkylation or Arylation	Acylation	Oxidation
cysteine	-CH_2SH	+	+	+
lysine	-NH_2	+	+	-
methionine	-S-CH_3	+	-	+
histidine	imidazolyl	+	+	+
tyrosine	-Ph-OH	+	+	+
tryptophan	indolyl	+	-	+
aspartic and glutamic acids	-COOH	-	+	-
arginine	-NHC(=NH)NH_2	-	-	-

Because protonation decreases the nucleophilicity of a species, the pH of the medium affects the rate of many nucleophilic reactions. The relationship between protonation and the pH depends on the pKa of the nucleophile. Table 2.5 lists the pKas of the reactive groups in free amino groups and in model peptides. Because the pKa is a function of temperature, ionic strength, and microenvironment of the ionizable group, the table reflects only the approximate values of these groups in proteins. Using these values, the ratio of protonated to deprotonated species at a certain pH can be calculated by the Henderson-Hesselbalch equation:

$$pH = pKa + \log\{[A^-]/[AH]\}$$

Table 2.5 pKa of some reactive groups in amino acids and model peptides.

Functional group	**Amino acid residue**	**pKa in free amino acid**	**pKa in model peptides**
α-COOH	C-terminal	1.8-2.6	3.1-3.7
β-COOH	aspartic acid	3.9	4.4-4.6
γ-COOH	glutamic acid	4.3	4.4-4.6
α-NH_3	N-terminal	8.8 – 10.8	7.6 – 8.0
-SH	cysteine	8.3	8.5-8.8
ε-NH_3^+	lysine	10.8	10.0-10.2
-NHC(=NH_2^+)NH_2	arginine	12.5	>12

Thus, at a fixed pH, the most reactive group is usually the one with the lowest pKa. Because of their differences in the pKa values, the degree of protonation of these amino acid side-chain groups at a certain pH provides a basis for differential modification. For example, at neutrality, the amino groups are protonated rendering them unreactive. For a selective reaction with the carboxyl group, the condition of an acidic pH should be selected. At higher pHs, other nucleophiles, particularly the thiol group, will react. As a consequence, it should be obvious that changing the pH also provides means to control the course of a chemical reaction.

2.3.3 Nucleophilic Substitution and Addition Reactions

Most of the protein modification reactions are nucleophilic substitution and addition reactions. For example, the reaction of succinimidyl esters with amino groups is an S_N2 substitution, while that of maleimidyl groups with thiols is a nucleophilic addition. The reaction rate of S_N2 substitution, a bimolecular nucleophilic substitution reaction, depends on the chemical reactivity of the involved species and the steric effects. The chemical reactivity involves the ability of the leaving-group to leave and the nucleophilicity of the attacking group. The easier it is for the leaving group to come off, the faster the reaction will be. Similarly, the greater the nucleophilicity, the more expeditiously the product will be formed. In term of protein modification, the relative chemical reactivity is basically a function of nucleophilicity of the amino acid side chains. On the other hand, the steric effects play a more important role on the surface reactions. Generally, in the bulk chemistry the less the bulky groups around the reactive target-atom, the easier the reaction will be. However on the surface, besides the native properties of molecules, the neighboring molecules also affect the steric hindrance. The denser the packed molecules, the more difficult the reaction will be. Therefore, a densely packed monolayer is not an ideal candidate for S_N2 surface reactions. Nucleophilic additions are accepted as stepwise reactions. They are classified to base- and acid-catalyzed additions. In order to avoid the side-reactions, the specific reaction of maleimidyl groups with thiols is often carried out under weakly acidic conditions.

2.3.4 Immobilization of RGD Peptides on Polymers [11]

In most cases, RGD peptides are linked to polymers via a stable covalent amide bond. This is usually done by reacting an activated surface carboxylic acid group with the nucleophilic N-terminus of the peptide. Carboxylic acid groups can be activated by using a peptide coupling reagent, e.g. 1-ethyl-3-(3-dimethylaminopropyl)-carbodiimide (EDC, also referred to as water soluble carbodiimide, WSC), dicyclohexyl-carbodiimide (DCC) or carbonyl diimidazole (CDI). Two problems may arise by this coupling method: Firstly there are further reactive functional groups in the RGD peptide (carboxyl groups at the C-terminus and in the aspartic acid side chain and the nucleophilic guanidino group of the arginine

side chain) and secondly the coupling reagent and the activated carboxyl groups can be deactivated quickly by hydrolysis. One possibility to overcome these problems is to block the reactive amino acid side chains with protecting groups and to use other solvents than water (e.g. DMF, dichloromethane or acetone). By this method, protected RGD peptides were successfully linked to polymers [12]. A major drawback of this immobilization strategy is the need of harsh conditions to remove the protecting groups. Even if the more labile Pbf (2,2,4,6,7-pentamethyl-dihydrobenzofurane-5-sulfonyl) protecting group for the arginine side chain is used, deprotection with trifluoroacetic acid (TFA) usually takes as long as 1–3 h. The malodorous deprotection mixtures can be replaced by using triethylsilane (TES) or triisopropylsilane (TIPS) as scavengers. Alternatively, coupling of unprotected RGD peptides in water is possible, employing a two step procedure: First, activation of the surface carboxyl group as an active ester that is less prone to hydrolysis, e.g. *N*-hydroxysuccinimide (NHS) esters, and second coupling of the peptide in water (Figure 2.9). NHS active esters on polymers are usually generated in dichloromethane or DMF, using DCC or EDC for activation of the carboxyl groups and subsequent reaction with NHS [13]. Alternatively, the TSTU reagent (*O*-(*N*-succinimidyl)-*N*,*N*,*N*',*N*'-tetramethyluronium tetrafluoroborate) reagent can be used, containing both the activation moiety as well as the NHS group. The half lifetime of NHS active esters at neutral pH ranges from several minutes to hours, depending on the substituents of the α-carbon [14]. NHS active esters that have been dried can be stored for several months [13, 14]. Best conditions for coupling the RGD peptide to the NHS active ester are pH 8–9 in phosphate or sodium bicarbonate buffer. Coupling is usually complete in 1–2 h. More elevated pH values and high concentrations of buffer or salts can reduce the half lifetime of the NHS active ester down to less than 1 min. Following this protocol, there is no need for protecting groups. Because of the two step procedure, the aspartate side chain carboxyl group is not activated for coupling, and due to protonation in water the nucleophilicity of the arginine side chain is nearly abolished. In some cases coupling was performed at lower pH and/or lower temperatures with longer coupling times resulting in higher yields. Also an excess of peptide may increase yields.

Creating NHS active esters in water using NHS and the water soluble coupling reagent EDC is also possible [15], but RGD peptide coupling yields are usually lower. In some cases the NHS active esters were introduced into the polymer by copolymerizing monomers that contain an NHS active ester. Polymers that contain surface amino groups can be treated with succinic anhydride to generate surface carboxyl groups, which can be reacted with RGD peptides as described above. Amino groups can directly be converted into preactivated carboxyl groups by using an excess of bisactivated moieties like disuccinimidyl tartate, disuccinimidyl suberate, ethylene glycol bis(succinimidyl succinate) (EGS) or *N*,*N*'-disuccinimidyl carbonate (DSC). Similarly bistresyl-PEG was used as a linker, leading to immobilized RGD peptide via amine bonds. Surfaces containing hydroxyl groups can similarly be preactivated with tresyl chloride (Figure 2.9). Alternatively hydroxyl groups can be treated with *N*,*N*'-disuccinimidyl carbonate or *p*-nitrophenyl chlorocarbonate to achieve activated material that either reacts readily with the peptide under aqueous conditions or can be stored for some time. Released *p*-nitrophenol upon coupling can be detected and quantified by UV absorption. *p*-Nitrophenol and tetramethylurea (from TSTU) are toxic and have to be removed carefully from the surfaces prior to biological applications.

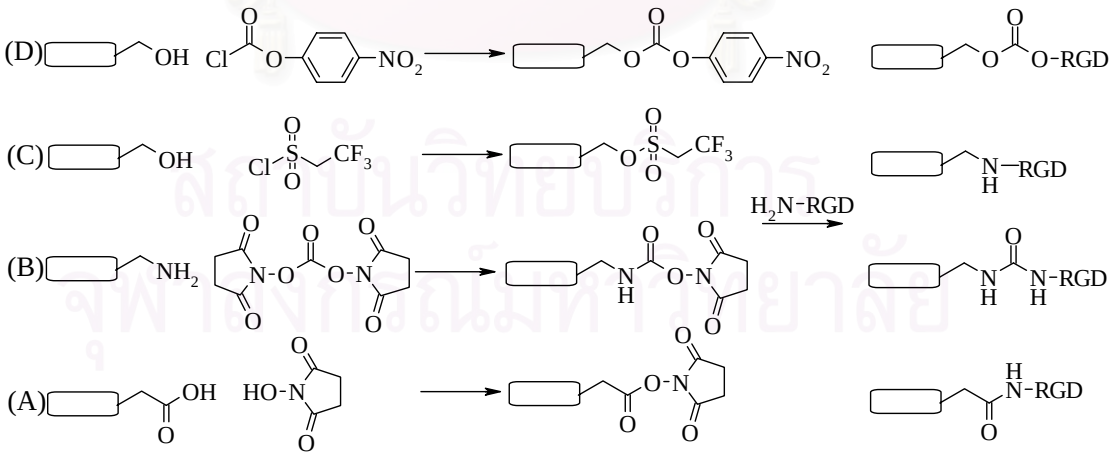

Figure 2.9 RGD peptides react via the *N*-terminus with different groups on polymers: (A) carboxyl groups, preactivated with a carbodiimide and NHS to generate an active ester, (B) amino groups, preactivated with DSC, (C) hydroxyl groups, preactivated as tresylate, (D) hydroxyl groups, preactivated as *p*-nitrophenyl carbonate.

In a more recent approach named chemoselective ligation, selected pairs of functional groups are used to form stable bonds without the need of an activating agent and without interfering with other functional groups. Chemoselective ligation proceeds usually under mild conditions and results in good yields. A bromoacetyl containing RGD cyclopeptide was successfully linked to a thiol functionalized surface and an aminooxy-terminated RGD cyclopeptide reacts readily with aldehyde groups leading to a stable oxime bond (Figure 2.10). Imine bonds resulting from coupling of a surface aldehyde group and the peptide's N-terminus have to be reduced to a more stable amine bond prior to application (''reductive amination''). Thiol (cysteine) bearing RGD peptides can be linked in a Michael addition reaction to acrylic esters or acryl amides in excellent yields [21]. In a similar addition reaction thiol containing RGD peptides were linked to maleinimide functionalized surfaces under mild conditions (Figure 2.10). The latter thiol reactive surface was created by reacting surface amino groups with a heterobifunctional linker, sulfo-SMCC (sulfosuccinimidyl 4-(*N*-maleinimidomethyl)cyclohexane-1-carboxylate). Also benzoquinone as a Michael type bifunctional linker between surface hydroxyl groups and the N-terminal amine was proposed. In some cases RGD peptides are immobilized by radical reactions. An acrylamide tailored RGD cyclopeptide was successfully immobilized on PMMA surfaces using camphorquinone and UV irradiation. Benzophenone as well as aromaticazide functionalized RGD peptides have been used to react similarly.

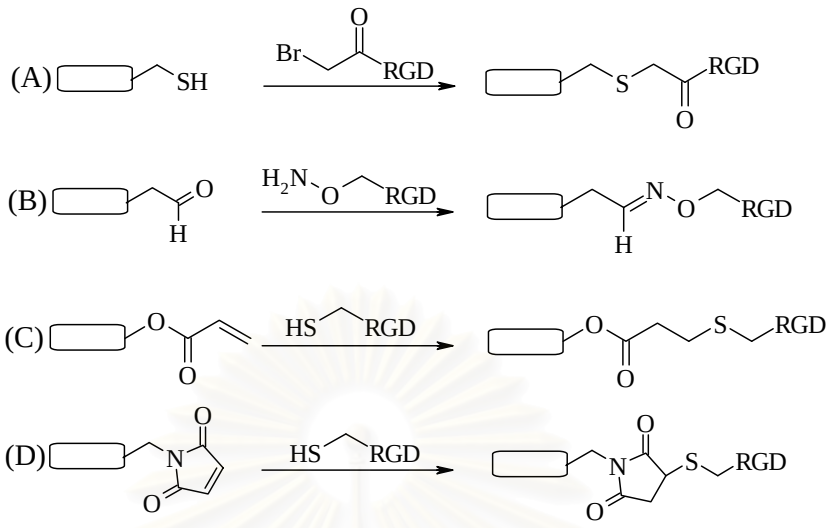

Figure 2.10 Chemoselective ligation of selected pairs of functional groups. (A) thiol and bromoacetyl-RGD. (B) aldehyde and aminooxy-RGD. (C) acrylate and thiol-RGD. (D) maleinimide and thiol-RGD.

In 1998, Xiao and coworkers design a surface modification method for covalent attachment of Arg-Gly-Asp (RGD)-containing peptides on Ti surfaces. The surface modification route is shown in Figure 2.11. Water-vapor-plasma-pretreated titanium surfaces were first activated by (3-aminopropyl)triethoxysilane (APTES), followed by reaction of terminal amines with succinimidyl esters of the crosslinkers, *N*-succinimidyl-6-maleimidylhexanoate, *N*-succimidyl trans-4-(maleimidyl-methyl)cyclohexane-1-carboxylate or *N*-succinimidyl-3-maleimidylpropionate. The final step involved the covalent binding of the thiol-bearing, RGD-containing peptides (glycine-arginine-glycine-aspatic acid-serine-proline-cysteine, GRGDSPC or arginine-glycine-aspatic acid-cysteine, RGDC) through maleimidyl groups. Infrared reflection absorption spectroscopy (IRAS), x-ray photoelectron spectroscopy (XPS) and radiolabelling technique were used for surface characterization. An approximate coverage of 0.2-0.4 peptides/nm^2 was calculated [16].

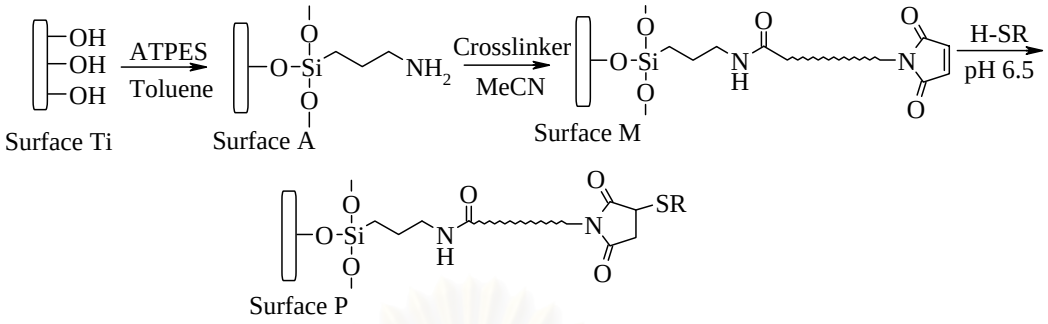

Figure 2.11 Schematic representation of the modification route. Surface Ti: water-vapor plasma-pretreated titanium; Surface A: poly(3-aminopropyl)siloxane pendant surface; Surface M: maleimide-modified surfaces with different alkyl chains; Surface P: peptide- or L-cysteine-modified surfaces; H-SR: L-cysteine, RGDC, GRGDSPC.

In 2001, Quirk and coworkers immobilized GRGDS peptide on the surfaces of poly(lactic acid)(PLA). Direct immobilization is impossible due to the lack of functional groups to support covalent attachment. They demonstrated a method to overcome this problem, by firstly attaching the peptide to poly(L-lysine) (PLL) using NHS/EDCI as a coupling agent to yield PLL-GRGDS. Bovine aortic endothelial cells seeded on the PLA coated with a 0.01% w/v solution of PLL-GRGDS showed a marked increase in spreading over unmodified PLA [12].

In 2002, Davis and coworkers modified silicon surface by RGD peptide attachment. Silicon surfaces coupled with a synthetic RGD peptide, as characterized by x-ray photoelectron spectroscopy (XPS) and atomic force microscopy (AFM), displayed enhanced fibroblast proliferation and bioactivity. Results demonstrate an almost three-fold greater cell attachment/proliferation on RGD immobilized surfaces compared to unmodified silicon surfaces [17].

In 2004, Yoon and coworkers immobilized glycine-arginine-glycine-aspatic acid-tyrosine, GRGDY onto the surface of highly porous biodegradable polymer scaffolds for enhancing cell adhesion and function. A carboxyl terminal end of poly(D,L-lactic-*co*-glycolic acid) (PLGA) was functionalized with a primary amine group by conjugating hexaethylene glycol-diamine. The PLGA-NH_2 was blended with PLGA in varying ratios to prepare films by solvent casting or to fabricate porous scaffolds by a gas foaming/salt leaching method. Under hydrating conditions, the

activated GRGDY could be directly immobilized to the surface exposed amine groups of the PLGA-NH_2 blend films or scaffolds. For the PLGA blend films, the surface density of GRGDY, surface wettability change, and cell adhesion behaviors were characterized. The extent of cell adhesion was substantially enhanced by increasing the blend ratio of PLGA-NH_2 to PLGA. The level of an alkaline phosphatase activity, measured as a degree of cell differentiation, was also enhanced as a result of the introduction of cell adhesive peptides [18].

2.4 Analysis of RGD-modified Polymers

Analysis of RGD-modified surfaces should answer the question of the presence of RGD peptides (qualitatively) and of the amount of the peptide in a certain area or volume of the polymer (quantitatively). Quantification is not only important to optimize RGD coupling conditions [19], but also to discover the effects of RGD surface density on cell response. Water contact angle analysis is a relatively simple method of characterizing surfaces. Smaller angles indicate an increased hydrophilicity of a solid surface and are usually detected when the zwitterionic RGD moieties are immobilized.

In a more specific approach, amide bonds on solid surfaces can be detected via ATR-FTIR (attenuated total reflection FTIR) at 1650 and 1530 cm^{-1}. If samples can be prepared as thin films, FTIR can be employed. In one case the rate of RGD coupling to a isocyanate functionalized surface was measured by quantifying a disappearing NCO band. X-ray photoelectron spectroscopy (XPS) is used to perform surface elemental analysis. Usually an enrichment of nitrogen and C=O carbons can be detected. By varying the take-off angle, vertical distribution of nitrogen as indicator for the peptide can be examined. If a specific elemental tag like fluorine or iodine is incorporated in the RGD peptide, XPS can be used for quantification [20].

Some more general methods for RGD peptide quantification include amino acid analysis (AAA) and radioassays. In AAA the whole surface is hydrolyzed, and the free amino acids are detected using standard amino acid analyzers [21]. Alternatively the hydrolysate can be quantified as a mixture by using the ninhydrin test and comparing its UV absorption values with calibrated controls.

Employing radioiodination very small amounts (fmol/cm^2) of peptides can be detected. Radioactivity is usually introduced in peptides by oxidative iodination of tyrosine. Thus Na^{125}I is used in combination with immobilized iodogen as oxidant. After purification of the iodinated peptide a certain amount of radioactivity is assigned to a certain amount of spectroscopically quantified peptide [20]. In some applications radioiodinated peptide was diluted with non-modified peptide prior to surface immobilization [21].

By using a gamma counter, surface density gradients of a radioiodinated RGD peptide could be detected. Indirect quantification of immobilized RGD peptide can be achieved by measuring the amount of unreacted soluble peptide, by using HPLC/UV detection, the TNBS (trinitrobenzene sulfonicac id) assay or Ellmans reagent for thiol containing peptides. Indirect quantification, however, leads only to results with reduced reliability. The Sakaguchi assay for detecting arginine groups and the BCA (bicinchonic acid) assay which is usually used for protein quantification [22] require careful calibration when applied for RGD quantification. Determining RGD densities by the amount of attached cells or by an ELISA, using Merck's anticyclo(RGDfK) antibody led only to semiquantitative but nevertheless useful results.

Detection of microdistribution of RGD peptides is a challenging task and has not been solved yet. The methods used so far include AFM or 2D ToF SIMS detection of bigger RGD containing moieties like comb copolymers and latex beads [20,23]. Microdistribution of RGD peptides could possibly be discovered by high resolution XPS or AFM using integrin or RGD antibody coated AFM tips.

2.5 Cell Surface and Cell Adhesion [23, 24]

Adhesive interactions enable individual cells to form and stabilize close contacts in order to maintain higher-order tissue specializations and facilitate information transfer. The study of cell adhesion is largely a study of individual adhesion molecules, which participate in a variety of cellular processes that include:

1. cell-cell recognition
2. maintenance of cell-contacts and tissue integrity
3. cell-signaling, information transfer and differentiation
4. cell-migration

Adhesive mechanisms are grouped into two major categories: cell-cell and cell-extracellular matrix adhesion.

1. Cell-cell adhesion involves "close" interactions (typically within 15-20 nm distances) at the cell-surface that are mediated by transmembrane and/or membrane-associated glycoproteins
2. Many cells interact with their extracellular environments by adhering to a "network" of secreted glycoproteins and other glycoconjugates, termed collectively extracellular matrix (ECM).
3. Multiple types of adhesive mechanisms are available to most cells. Some of these mechanisms are functionally redundant (i.e., compensatory).

The view of the cell surface has been modified in recent years by the realization that the cytoskeleton is often physically associated with adhesion molecules at the cell surface. Some of these adhesion molecules function as transmembrane linking between the cytoskeleton and the ECM.

The Molecular Basis for Cell Adhesion

Cells use 4 basic types of molecular interactions to adhere:

1. Homophilic adhesion involves the binding of adhesion molecules on the surface of one cell to the same kind of adhesion molecules on another cell.

2. Heterophilic adhesion involves the binding of adhesion molecules on one cell to adhesion molecules of a different kind on another cell.

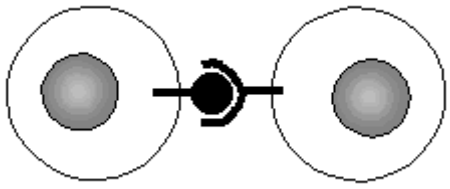

3. Cells can also bind to one another indirectly, by adhering to an extracellular "intermediate" (e.g., an ECM linker molecule).

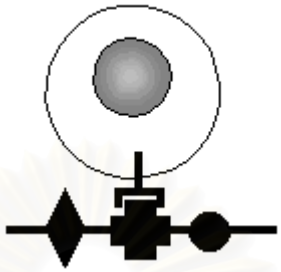

4. Cell-substrate adhesion involves the binding of a cell-surface receptor to a secreted ECM molecule immobilized on the substrate.

Many cell adhesive interactions can be further distinguished by their requirements for divalent cations. For example, some adhesion molecules require Ca^{++} or Mg^{++} for function.

Several families of cell surface receptor molecules function in cell-cell and cell-ECM adhesion. Although structurally distinct, representatives from each of these families share a number of common features. They are all transmembrane proteins, which have large extracellular ligand-binding domains and relatively short cytoplasmic domains. The four most widely studied and functionally important groups of adhesion molecules are the immunoglobulin-superfamily (IgSF), and the cadherin (CAD), selectin, and integrin families.

1. Cadherins require Ca^{++} for adhesive function and are involved in homophilic cell-cell adhesion. Members of the cadherin family are expressed in specific tissues during development where they are believed to play important roles in morphogenesis. Cells expressing different CADs will “sort out” into homotypic (tissue-specific) aggregates under appropriate experimental conditions. E-cadherin (E-CAD) is a critical component of the zonula adherens junction. E-CAD links adjacent epithelial cells together and colocalizes with “bands” of actin filaments that encircle each epithelial cell. Loss of E-CAD is associated with many cancers of epithelial origin.

2. Selectins are adhesion molecules that mediate a variety of heterophilic interactions among leukocytes and endothelial cells that are important in inflammation and

immune response. Selectins are characterized by a single Ca^{++}-dependent lectin domain, which binds to specific carbohydrate groups on adjacent cells.

3. The immunoglobulin superfamily (IgSF) includes a number adhesion receptors characterized by the presence of large extracellular globular-domains held in place by disulfide bonds. IgSF receptors do not require divalent cations for adhesive function. Most, but not all, members of this family are involved in homophilic cell-cell adhesion and are thought to play important roles in embryonic development. I-CAM is a member of the IgSF that is expressed on activated endothelial cells where it is involved in heterophilic cell-cell adhesion. I-CAM binds to integrin counter-receptors expressed on leukocytes (white blood cells).

4. The integrins function as cellular receptors for many ECM glycoproteins. They provide a transmembrane linkage between the ECM and the cytoskeleton. Integrins have several important features and functions:

a. Integrins are heterodimers composed of 2 distinct glycocoprotein subunits termed α and β. The α subunit binds divalent cations (e.g., Ca^{++}), which are essential for integrin ligand binding function.
b. The integrins comprise a large family of closely related receptor complexes. Different αβ subunit combinations differ in their ligand binding specificities and affinities. A large number of α subunits combine with a relatively smaller number of β subunits to yield multiple receptors. Some integrins specifically recognize only one ligand while others can interact with multiple ligands. Considerable functional “redundancy” is apparent in members of the integrin family.
c. Integrin-dependent adhesion can stimulate cell-signaling pathways important in regulating cell-growth, survival and gene expression
d. Not all integrins are involved in cell-ECM adhesion. Some integrins are involved in heterophilic cell-cell adhesion (e.g., by binding select IgSF receptors)

The ECM also plays an indirect role in cell-cell adhesion. Unlike the close contacts mediated by CAMs, CADs and Selectins, ECM molecules provide an intercellular "scaffold" to which cells adhere.

CHAPTER III

EXPERIMENTAL

3.1 Materials

All reagents and materials are analytical grade and use without further purification

1. Acetic acid : Merck
2. Bromine : Fluka
3. Chloroform-d : Aldrich
4. Deuterium oxide : Aldrich
5. Dicyclohexyl carbodiimide (DCC) : Fluka
6. Diethylether : Merck
7. 1,4-Dioxane : Merck
8. Ethanol : Merck
9. 1-Ethyl-3-(3-dimethylaminopropyl)carbodiimide : Fluka
10. Fibroblast cell line (B95) : Allergy and Clinical Immunology Unit, Faculty of Medicine, Chulalongkorn University
11. H-Arg-Gly-Asp-OH : CalBiochem
12. H-Arg-Gly-Asp-Ser-OH : CalBiochem
13. H-Gly-Arg-Gly-Asp-Ser-OH : CalBiochem
14. Heptafluorobutyryl chloride : Aldrich
15. *N*-hydroxysuccinamide (NHS) : Fluka
16. Isopropyl alcohol : Merck
17. L-tyrosine : Fluka
18. Methanol : Merck
19. Methylene chloride : Merck

20. Ninhydrin : Merck
21. Phosphate buffer saline (PBS) : Aldrich
22. Poly(DTE-*co*-20%DT carbonate) Mw 81126 : The New Jersey Center For Biometerials
23. RPMI 1640 : Gibco
24. Sodium metabisulphite : Unival
25. Tetrahydrofuran : Merck
26. Triethylamine : Merck
27. Trypsin-EDTA solution : Gibco

3.2 Equipments

3.2.1 Nuclear Magnetic Resonance (NMR)

The ^{1}H and ^{13}C NMR spectra were recorded in either $CDCl_3$, D_2O or DCl using a Bruker, model AC-F200, Avance DPX-400 and Varian, model Mercury-400 nuclear magnetic resonance spectrometer operating at 400 MHz. Chemical shifts (δ) are reported in part per million (ppm) relative to tetramethylsilane (TMS) or using the residual protonated solvent signal as a reference.

3.2.2 Contact Angle Measurements

Contact angle meter model FACE, Japan was used for the determination of water contact angles. A droplet of testing Milli-Q water is placed on the tested surface by bringing the surface into contact with a droplet suspended from a needle of the syringe. The measurements were carried out in air at the room temperature. Dynamic advancing and receding angles were recorded while water was added to and withdrawn from the drop, respectively. The reported angle is an average of 5 measurements on different area of each sample.

3.2.3 X-ray Photoelectron Spectroscopy (XPS)

X-ray photoelectron spectra were collected using ESCA-200, SCIENTA, Uppsala, Sweden. In this study, the take off angle at 15° and 90° were chosen and the approximate of depth profile is ~10 Å and ~40 Å, respectively.

3.2.4 Attenuated Total Reflectance-Fourier Transform Infrared Spectroscopy (ATR-FTIR)

All spectra were collected at resolution of 4 cm^{-1} and 64 scan using Bruker vector 33 FT-IR spectrometer equipped with a DTGS detector. A single attenuated total reflection accessory with 45° zinc selenide (ZnSe) IRE (spectra Tech, USA) and a varible angle reflection accessory (Seagull^{TM}, Harrick Scientific, USA) with a hemispherial ZnSe IRE were employed for all ATR spectral acquisitions.

3.2.5 UV-Spectroscopy

UV spectroscopy Model Techna, specgene was used for determination the amount of amino groups on poly(DTE-*co*-20%DT carbonate) surface after RGD immobilization using ninhydrin method by reading UV absorbance at 538 nm.

3.2.6 Hemocytometer

The Hemocytometer is a cheap and effective way to count cells. This apparatus is basically a microscope slide consisting of an optically flat chamber. A coverslip is then place securely over the chamber thereby determining its depth. A known volume (20μL) of a homogenous cell suspension is then drawn into the chamber by capillary action. The microscope is used to focus on a defined grid area of dimension $1mm^2$ and the numbers of cell in the area counted.

In order to achieve an accurate cell count it is essential that the suspended cells are homogenous and devoid of aggregation. It is also important to transfer the cells from gilsen tip to chamber as quickly as possible to avoid the settling or adhering of cells to tip.

Ideally the numbers of cells should be between 100-300/mm^2 in order to provide a reasonable degree of accuracy. The greater the number of cells the better. Counts of both chambers should be taken and average calculated.

The number of cells is calculated using the formula below:-

$$c = n/v$$

Where c – cell concentration(cells/mL)

n – number of cells counted

v – volumn counted(mL)

The Improved Neubauer Slide which has a depth of chamber of 0.1mm is used. Therefore using the count area of $1mm^3$ (or $10^{-4}cm^3$). Rearranging the above formula in light of this information gives:-

$$C = n \times 10^4$$

Therefore if there is an average cell count (n) of 200 then the cell concentration will be 200×10^4 which is equivalent to 2,000,000 cells/mL. The total numbers of cells present can be simply calculated by multiplying c by the original volume of suspended cells.

3.2.7 Statistical Analysis

Values are expressed as the mean ± SD. Experiments were performed at least five times and results of representative experiments are presented except where otherwise indicated. Statistical analysis was performed using one-way analysis of variance (ANOVA) with the Student-Newman-Keul's test (SNK) multiple comparisons posttest using SPSS 10.0.1 software. $p<0.01$ or $p<0.05$ was considered statistically significant.

3.3 Methods

3.3.1 Activation of Poly(DTE-*co*-20%DT carbonate) with *N*-hydroxysuccinimide under Homogeneous Condition

Poly(DTE-*co*-20%DT carbonate) 0.44 g in 10 mL of 10% methanol in methylene chloride (10 mL) was added into a 25 mL round bottom flask containing a magnetic bar. 0.029 g (0.25 mmole) of *N*-hydroxysuccinimide (NHS) and 0.052 g (0.25 mmole) dicyclohexyl-carbodiimide (DCC) were added. After reacting for 24 h at ambient temperature, precipitated dicyclohexyl urea was filtered and the solution was concentrated by evaporation. The white solid product was dried under vacuum.

3.3.2 Preparation of Poly(DTE-*co*-20%DT carbonate) Films

Poly(DTE-*co*-20%DT carbonate) sample (2.0 g) was dissolved in 20 mL of 10% methanol in dichloromethane. The solution was filtered by PTFE membrane (1.0 μm pore diameter) before cast into a glass mold (10x10 cm^2) coated with Teflon.

Solvent was allowed to evaporate under N_2 atmosphere overnight. The film was dried under vacuum for 2 days.

3.3.3 Activation of Poly(DTE-*co*-20%DT carbonate) with *N*-hydroxysuccinimide under Heterogeneous Condition

Poly(DTE-*co*-20%DT carbonate) film (5x5 mm^2) was treated with a carbodiimide solution (0.1 M 1-ethyl-3-(3-dimethylaminopropyl) carbodiimide hydrochloride (EDCI) and 0.1 M *N*-hydroxysuccinimide (NHS)) in 5 mL selected solvent at ambient temperature for a certain period of time. After rinsed twice with ethanol, the activated poly(DTE-*co*-20%DT carbonate) film was dried under vacuum overnight.

3.3.4 Synthesis of L-3,5-Dibromotyrosine

0.9 g L-bromotyrosine was dissolved in 1 mL of glacial acetic acid and 9 mL of water. The solution was added dropwise to the solution of 0.64 mL of bromine in 3 mL of glacial acetic acid in an ice bath. Sodium metabisulphite (NaS_2O_5) was then added to the solution until the color of bromine disappeared. After pH of the solution was adjusted to 7, the product was isolated by filtration, washed thoroughly with cool deionized water and dried under vacuum.

H-NMR (DCl): δ 2.9 (2H, PhOHC$\underline{H}_2$, m, J = 5.86Hz, J = 7.62Hz) δ 4.03 (1H, PhOHCH$_2$C$\underline{H}$NH_2, t), δ 7.2 (2H, Ar$\underline{H}$CH_2, s)

3.3.5 Reaction of Activated Poly(DTE-*co*-20%DT carbonate) Film with L-3,5-Dibromotyrosine

L-3,5-dibromotyrosine was dissolved in a solution of 2 mL DMF and 3 mL phosphate buffer solution (pH = 7.4). The activated poly(DTE-*co*-20%DT carbonate) film was added to the solution. After reacting for 2 h, the film was rinsed twice with phosphate buffer solution (pH = 7.4) and deionized water, respectively. The film was dried under vacuum overnight. -

3.3.6 Reaction of Activated Poly(DTE-*co*-20%DT carbonate) Film with RGD-containing Peptide

RGD-containing peptide (RGD, RGDS or GRGDS; 0.05 M) was dissolved in phosphate buffer solution (pH = 7.4). The activated poly(DTE-*co*-20%DT carbonate) film was added to the solution. After reacting for 24 h, the film was rinsed twice with phosphate buffer solution (pH = 7.4) and deionized water, respectively. The film was dried under vacuum overnight.

3.3.7 Labeling of Immobilized RGD-containing Peptide by Heptafluorobutyryl chloride

Diethyl ether (10 mL) was added into a Schlenk flask containing an activated poly(DTE-*co*-20%DT carbonate) film. Triethylamine (0.070 mL, 0.05 mol) and heptafluorobutyryl chloride (0.075 mL, 0.05 mol) were added into the Schlenk flask via syringe. The solution was stirred at room temperature under nitrogen atmosphere for 24 h. Then the films were rinsed twice with diethyl ether and ethanol, respectively. The film was dried under vacuum overnight.

3.3.8 Determination of the Amino Groups on Poly(DTE-*co*-20%DT carbonate) Surface after RGD Immobilization

The ninhydrin analysis method was employed to quantitatively detect the amount of NH_2 groups on the RGD-immobilized poly(DTE-*co*-20%DT carbonate) film. The film was immersed in 1.0 mol/L ninhydrin/ethanol solution for 1 min and then placed into a glass tube, following with heating at 80 °C for 15 min to accelerate the reaction between ninhydrin and amino groups on the film. After the adsorbed ethanol had evaporated, 0.5 mL of 1,4-dioxane was added into the tube to dissolve the film when the film surface appeared blue. Another 0.5 mL of 2-propanol was added to stabilize the blue compound. The absorbance at 538 nm of this mixture was measured on a UV-vis spectrophotometer. A calibration curve was obtained with 1,6-hexanediamine in 1,4-dioxane/isopropanol (1:1, v:v) solution.

3.3.9 Cell Study

96-well cell culture plates were employed for cell study. Both modified and unmodified poly(DTE-*co*-20%DT carbonate) films (diameter: 6 mm) were transferred to cover the bottom of wells. 6 replicated samples were used for each condition. The seeding density of the fibroblast cell line (B95) was 25,000 cells/cm^3. Cells were cultured in RPMI 1640 medium containing 10% fetal bovine serum (FBS) and incubated under 5% CO_2 at 37^{o}C. As a control, the B95 were also directly seeded on tissue culture polystyrene substrate (TCPS) of plates. Medium was replaced 48 h after starting the culture and every 48 h thereafter.

After 12 h of incubation, the B95 were digested and isolated with 0.25% trypsin-EDTA for 10 min. Cells were counted with a hemocytometer, and the cell adhesion on each surface was evaluated using the equation shown below where $N_{\text{sample, 12 h}}$ represents the cell number on the different polymeric surfaces and $N_{\text{TCPS, 12 h}}$ represents the cell number on TCPS surfaces, which was utilized as a standard.

$$\% \text{ Cell adhesion ratio (CAR)} = \frac{N_{sample,12h}}{N_{TCPS,12h}} \times 100$$

The measurement of change in number of proliferated cells on modified and unmodified poly(DTE-*co*-20%DT carbonate) films was determined at the time point of 48 and 96 hours. Approximately 5 x 10^3 fibroblasts in 0.2 mL culture medium were pipetted into each well of 96-well tissue culture dishes containing the modified and unmodified poly(DTE-*co*-20%DT carbonate) films. Culture medium was replaced with fresh medium every 48 h while the cells were incubated, After designated incubation time, the films were rinsed with 0.2 mL phosphate buffer solution (pH = 7.4) to remove unattached cells and incubated with 0.25% trypsin-EDTA for 10 min to remove attached cells. Next, trypsin was neutralized with 0.2 mL phosphate buffer solution (pH = 7.4). Cells were counted with a hemocytometer.

CHAPTER IV

RESULTS AND DISCUSSION

The aim of this work is to covalently attach Arg-Gly-Asp (RGD)-containing peptides on poly(DTE-*co*-20%DT carbonate) surface, employing a two-step procedure. The first step involved an activation of surface carboxyl group into active *N*-hydroxysuccinimide (NHS) ester that is less prone to hydrolysis. The second step was a coupling of RGD-containing peptide. The mechanism of the activation of carboxyl groups on the surface followed by the coupling reaction with RGD-containing peptide is shown in Figure 4.1.

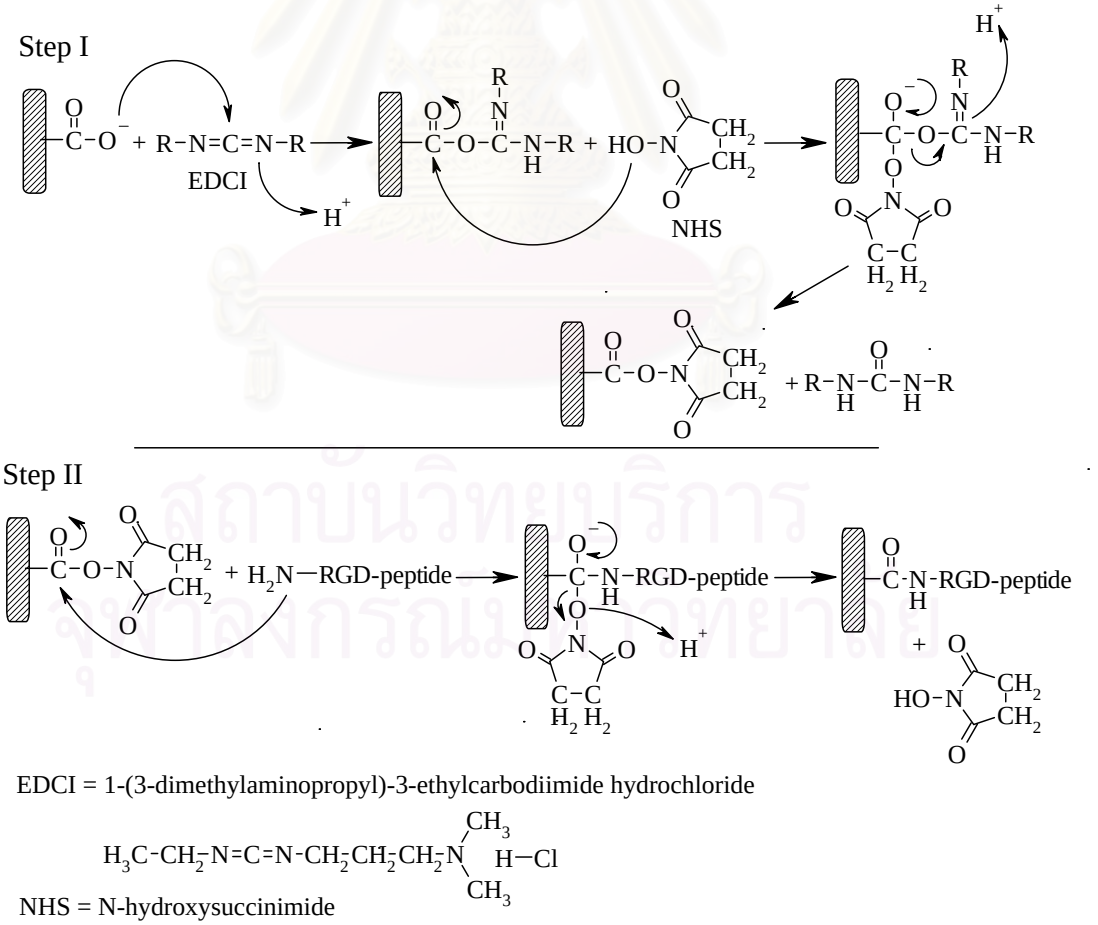

Figure 4.1 Mechanism of an activation of surface carboxyl group followed by a coupling reaction with RGD-containing peptide.

4.1 Activation of Poly(DTE-*co*-20%DT carbonate) with *N*-hydroxysuccinimide under Homogeneous Condition

The activation reaction was first conducted under homogeneous condition in order to determine a possibility to follow an extent of activation using ^{1}H NMR. Two solvent systems that can completely solubilize poly(DTE-*co*-20%DT carbonate) were chosen: 10% (v/v) methanol/methylene chloride and tetrahydrofuran.

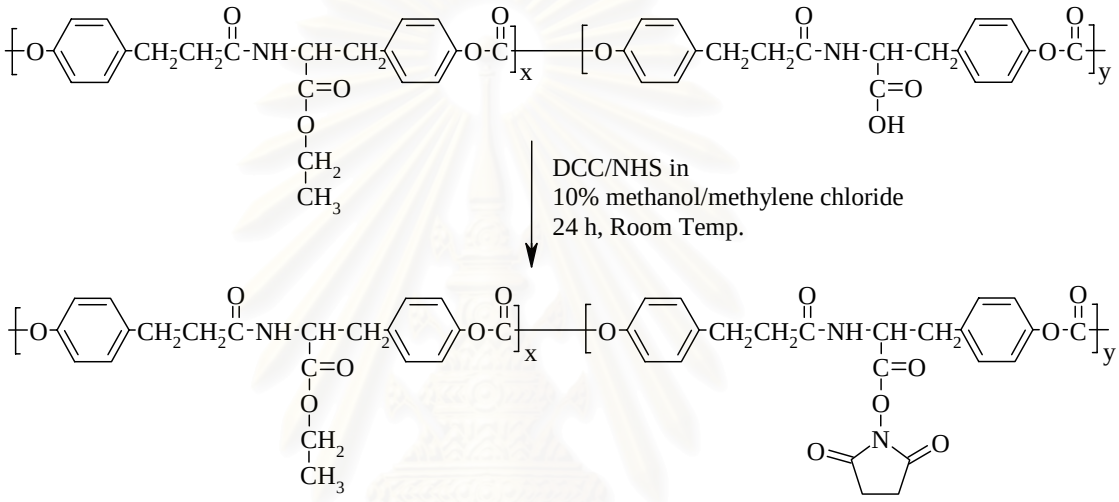

poly(DTE-*co*-20%DT carbonate), [y/(x+y)] x 100 = 20%

The activation reaction was carried out using 0.25 M *N*-hydroxysuccinimide (NHS) in the presence of 0.25 M dicyclohexylcarbodiimide (DCC) at room temperature for 24 h. According to Figure 4.2, there were significant changes of signals from ^{1}H NMR spectrum of virgin poly(DTE-*co*-20%DT carbonate) to the activated ones. A group of new peaks appearing in the range of 3.4-3.8 ppm and in the range of 1.8-2.0 can be assigned to dicyclohexylurea (DCU) which is a solid by-product of reaction. The urea precipitate cannot be completely removed even after filtration through PTFE membrane having 1.0 μm pore diameter. A signal at 2.85 ppm which is not present in ^{1}H NMR spectrum of virgin poly(DTE-*co*-20%DT carbonate) was labeled as protons of *N*-succinimide esters attached to carboxyl groups of the polymer. While a signal at 2.76 ppm corresponded to the unreacted NHS that was trapped inside the polymer. This study has demonstrated that it is possible to follow the extent of activation using ^{1}H NMR analysis since the signal of reacted NHS was well separated from the one of unreacted NHS. The extent of activation in

term of % substitution can be calculated from the relative peak area at 2.85 ppm belonging to the protons of *N*-succinimide and those binding to the α-carbon of tyrosine in the range of 4.76-4.84 ppm according to the following equation

$$\% \text{ Substitution} = \frac{\text{Integration of protons at 2.85 ppm}/4}{\text{Integration of protons in range of 4.76-4.84 ppm}} \times \frac{100}{\%DT}$$

The fact that the relative ratio of integration of protons at 2.85 ppm and the one of protons at 2.76 ppm obtained from 10% (v/v) methanol/methylene chloride is quite similar to the one obtained from tetrahydrofuran implies that the activated carboxyl groups in the form of *N*-succinimide esters are quite stable even in the presence of methanol which is a protic solvent.

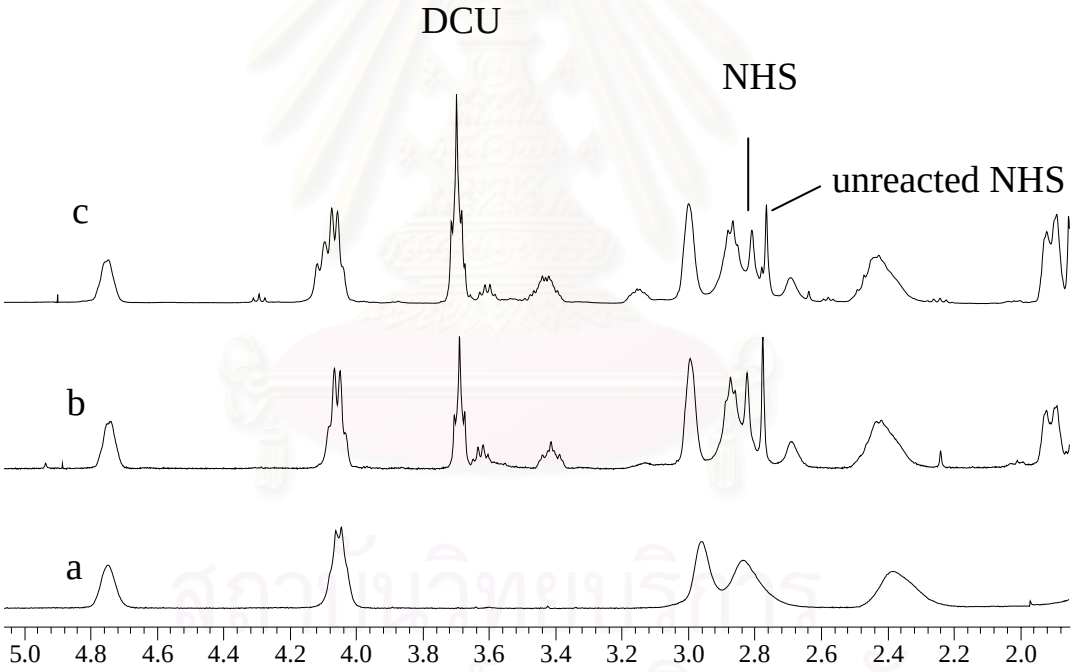

Figure 4.2 ^{1}H NMR spectra of (a) poly(DTE-*co*-20%DT carbonate) and poly(DTE-*co*-20%DT carbonate) after reacted with *N*-hydroxysuccinimide in (b) tetrahydrofuran and (c) 10% (v/v) methanol/methylene chloride.

4.2 Activation of Poly(DTE-*co*-20%DT carbonate) with *N*-hydroxysuccinimide under Heterogeneous Condition

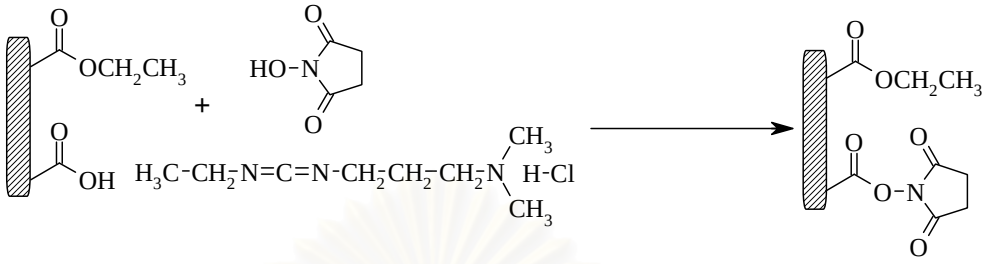

In light of the success of the activation conducted under homogeneous condition, the activation of carboxyl groups on the surface of poly(DTE-*co*-20%DT carbonate) with *N*-hydroxysuccinimide under heterogeneous condition was then pursued. In stead of using DCC, 1-ethyl-3-(3-dimethylaminopropyl)carbodiimide (EDCI) was used together with NHS for the heterogeneous reaction. Effects of solvent, concentration of coupling agent (NHS and EDCI) and reaction time on the extent of activation were investigated. ^{1}H NMR was used as a major tool for characterization while water contact angle measurement and ATR-FTIR were used in some cases. A series of experiments was conducted in order to determine the optimum condition for the activation of carboxyl groups on the surface of poly(DTE-*co*-20%DT carbonate) prior to an attachment with RGD-containing peptides.

4.2.1 Effect of Solvent

In principle, the success of chemical reaction at the polymer/solution interface is determined by the ability of solvent to wet and/or swell the polymer surface. According to literatures, the covalent attachment of RGD-containing peptides are generally performed in aqueous solution due to the fact that water can dissolve peptides as well as coupling reagents, NHS/EDCI in this particular case, and also wet the hydrophilic polymer substrate to some extent. For this reason, water was selected as the first solvent to be investigated. According to Figure 4.3, the water contact angle has increased from 71.5^{o}/29.8^{o} of the virgin poly(DTE-*co*-20%DT carbonate) film to the maximum of ~81.7^{o}/32.6^{o} of the activated film after 150 min of reaction in aqueous solution of 0.1 M NHS/EDCI. The contact angle did not increase any further after 150 min implying that the highest extent of activation in the surface region has

been achieved. This elevation of contact angle suggests that the hydrophilic carboxyl groups have been converted to hydrophobic *N*-succinimide groups.

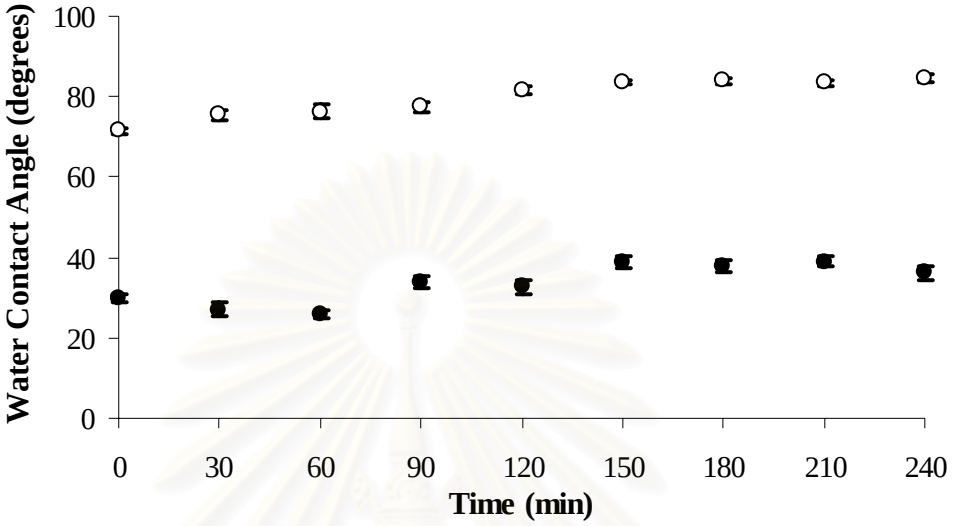

Figure 4.3 Water contact angle of poly(DTE-*co*-20%DT carbonate) film after the reaction with aqueous solution of 0.1 M NHS/EDCI: advancing (○) and receding (●).

The activated poly(DTE-*co*-20%DT carbonate) film obtained after the reaction between poly(DTE-*co*-20%DT carbonate) film and aqueous solution of 0.1 M NHS/EDCI was also characterized by ATR-FTIR. An emerging weak shoulder at 1825 cm^{-1} observed in the spectrum of the activated poly(DTE-*co*-20%DT carbonate) can be assigned to the the C=O stretching of succinimidyl ester (Figure 4.4). This result implied that the activation in aqueous solution has in fact proceeded at least to the sampling depth of ATR-FTIR (1-2 μm).

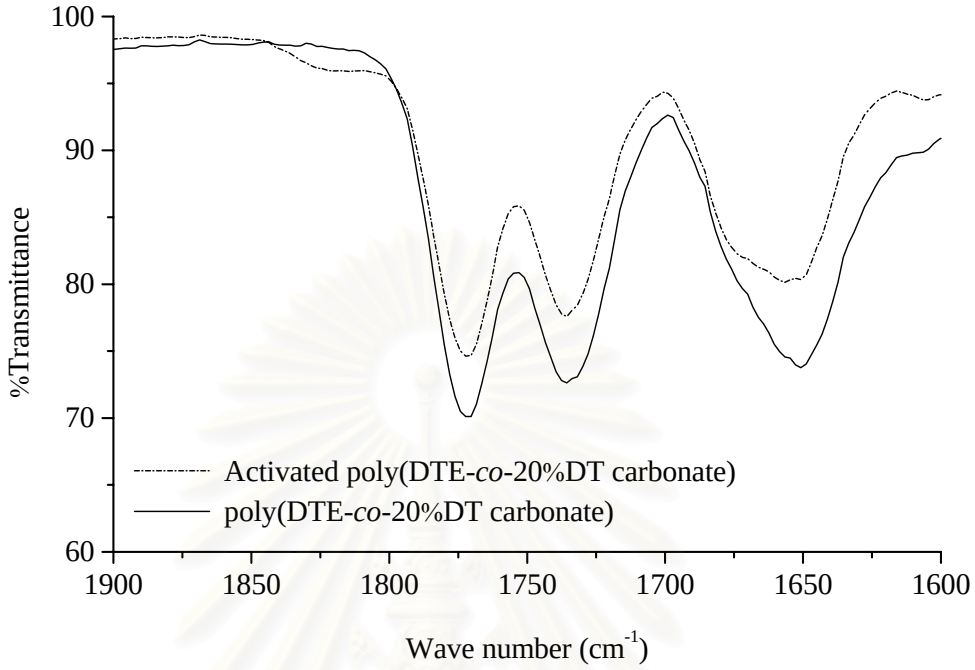

Figure 4.4 ATR-FTIR spectra of poly(DTE-*co*-20%DT carbonate) and activated poly(DTE-*co*-20%DT carbonate) films.

In order to quantitatively determine the extent of activation, the activated film was analyzed by ^{1}H NMR analysis. From Figure 4.5 (a), it turned out that there was no signal at 2.85 ppm which represents the protons of *N*-succinimide groups attached to the polymer. This may be explained by the fact that ^{1}H NMR analysis is a bulk characterization technique so it cannot assess any changes of functionality unless the activation has proceeded to a sufficient depth. In addition, water may not be able to swell the surface of poly(DTE-*co*-20%DT carbonate) film that well. As a consequence, the depth of activation was quite thin. For these reasons, ethanol was proportionally added to the aqueous solution of NHS/EDCI in order to increase the swelling of poly(DTE-*co*-20%DT carbonate).

The ^{1}H NMR spectra shown in Figure 4.5 (b-d) indicated that an extensive swelling of poly(DTE-*co*-20%DT carbonate) was necessary for the reaction to proceed deep enough so that the success of surface activation can be followed by ^{1}H NMR. This is the reason why the signal at 2.85 ppm was only detected when ethanol

was used as a solvent since it can swell the polymer much more extensively than the solvent mixtures between water and ethanol. Even though water contact angle and ATR-FTIR data can be used as indications of surface activation, they are not suitable for quantitative analysis. For the subsequent investigation, ethanol was thus used as a solvent to assure that the surface activation can proceed deep enough in the polymer film. The fact that the peak at 2.85 ppm previously assigned to the unreacted NHS was absent help demonstrating an advantage of using heterogeneous condition for activation. Since the reaction only took place on the surface, there was less chance for DCU or unreacted NHS to be trapped inside the polymer. If there were some, they should be insignificantly small and can be easily removed.

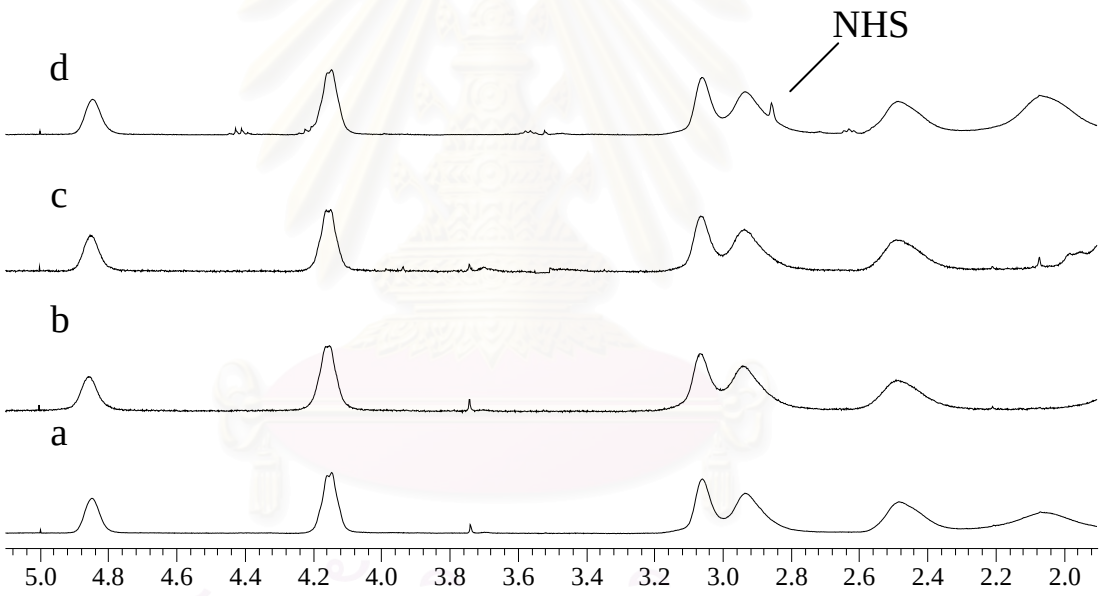

Figure 4.5 ^{1}H NMR spectra of poly(DTE-*co*-20%DT carbonate) film after the reaction with 0.1 M NHS/EDCI in (a) water, (b) 20% ethanol/water, (c) 50% ethanol/water and (d) ethanol for 2 h.

4.2.2 Effect of NHS/EDCI Concentration

Using ethanol as a solvent, %yield of activation calculated from the relative integration of the peak at 2.85 ppm corresponding to the proton of *N*-hydroxysuccinimide and the integration of the peak in the range of 4.76-4.84 ppm corresponding to the α-carbon of tyrosine was linearly increased as a function of

NHS/EDCI concentration (Figure 4.6). It is worth noting that the calculated % substitution was an average yield throughout the bulk because ^{1}H NMR analysis is a bulk characterization technique. It may not represent an actual reaction yield at the surface which could be considerably higher. It is suspected that increasing the NHS/EDCI concentration should promote the activation to proceed much deeper into the bulk resulting in higher overall yield which may or may not be relevant to the surface yield. Therefore, it is also possible that % substitution of activation in the surface region may reach its maximum without having to use a high concentration of NHS/EDCI.

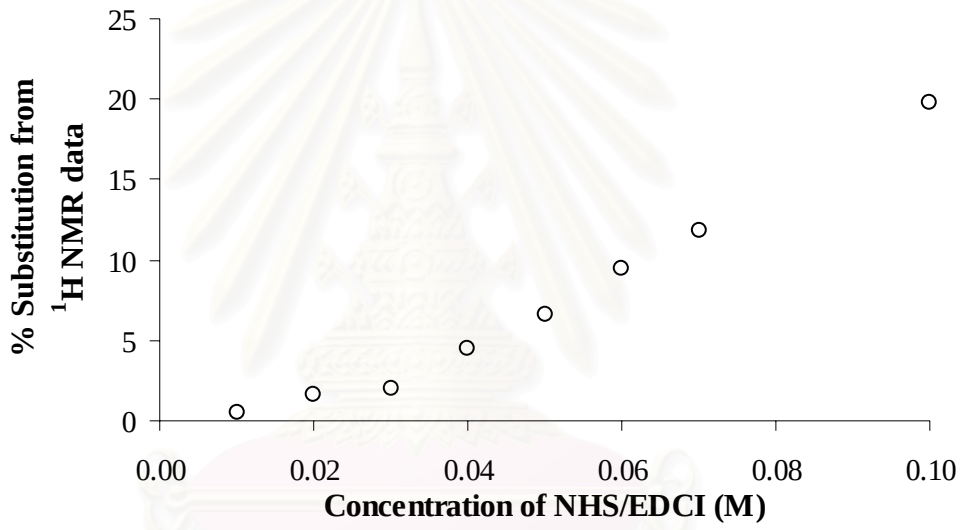

Figure 4.6 % Substitution of activation of poly(DTE-*co*-20%DT carbonate) film after reaction with NHS/EDCI solution in ethanol for 2 h as a function of NHS/EDCI concentration

4.2.3 Effect of Reaction Time

Choosing the moderate (0.05 M) and highest (0.1 M) concentration of NHS/EDCI used in the previous section, an effect of reaction time on % substitution of activation was investigated. As shown in Figure 4.7, % substitution of reaction was increased as a function of reaction time within the first 2 h of reaction for both cases. The maximum substitution of 8% and 20% were obtained using the NHS/EDCI concentration of 0.05 M and 0.1 M, respectively.

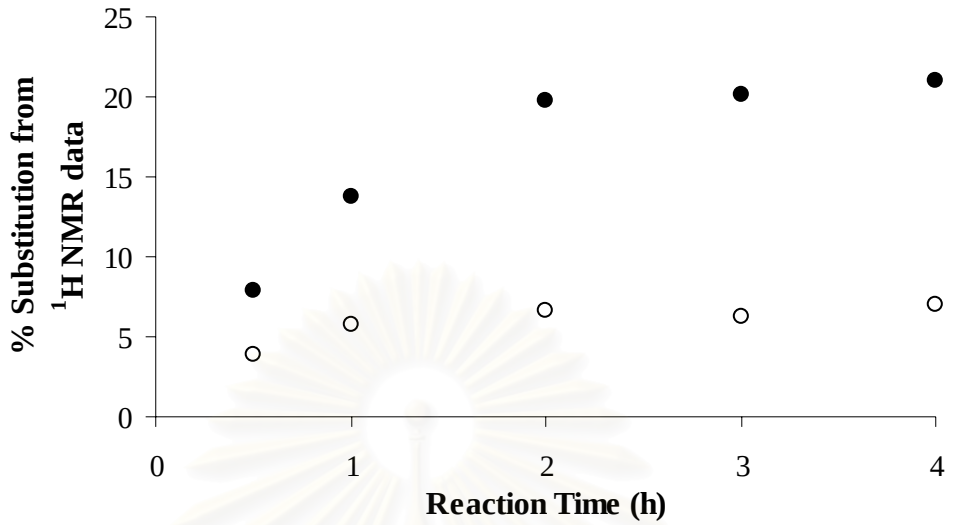

Figure 4.7 % Substitution of activation of poly(DTE-*co*-20%DT carbonate) film after the reaction with a varied concentration of NHS/EDCI solution in ethanol as a function of reaction time**:** 0.1 M (●) and 0.05 M (○).

An optimum condition for the preparation of NHS-activated poly(DTE-*co*-20%DT carbonate) film that can be deduced from ^{1}H NMR data is to use 0.1 M NHS/EDCI in ethanol and carrying out the activation for 2h

4.3 Reaction of Activated Poly(DTE-*co*-20%DT carbonate) Film with L-3,5-Dibromotyrosine

Prior to immobilization of RGD-containing peptides, the activity of *N*-succinimide groups on the polymer surface towards the substitution of amino groups of a model compound was first tested. L-3,5-Dibromotyrosine was selected as a model compound for peptide. Bromine was introduced to L-tyrosine as a tag element so the success of the model compound attachment can be followed by X-ray photoelectron spectroscopy (XPS), a surface characterization technique that can probe an atomic composition of surface within a sampling depth of up to 50 Å

4.3.1 Synthesis of L-3,5-Dibromotyrosine

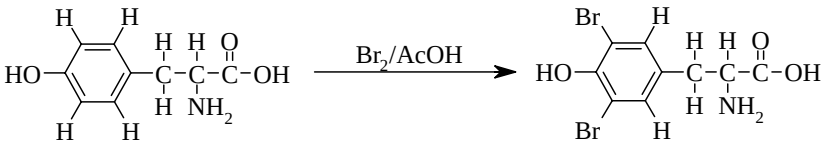

As a consequence of *ortho* and *para*-directing activation of hydroxyl group attached to an aromatic ring of L-tyrosine, the reaction between L-tyrosine and excess Br_2 *via* electrophilic aromatic substitution yielded a disubstituted product of L-3,5-dibromotyrosine. The substitution only occurred at two *ortho* positions of the hydroxyl group since the para position was not available. ^{1}H NMR spectrum of L-3,5-dibromotyrosine is shown in Figure 4.8. Two doublet signals from aromatic ring of L-tyrosine at 6.90 ppm and 7.19 ppm were replaced by a singlet signal at 7.18 ppm after bromination confirming the disubstitution of bromine in aromatic ring.

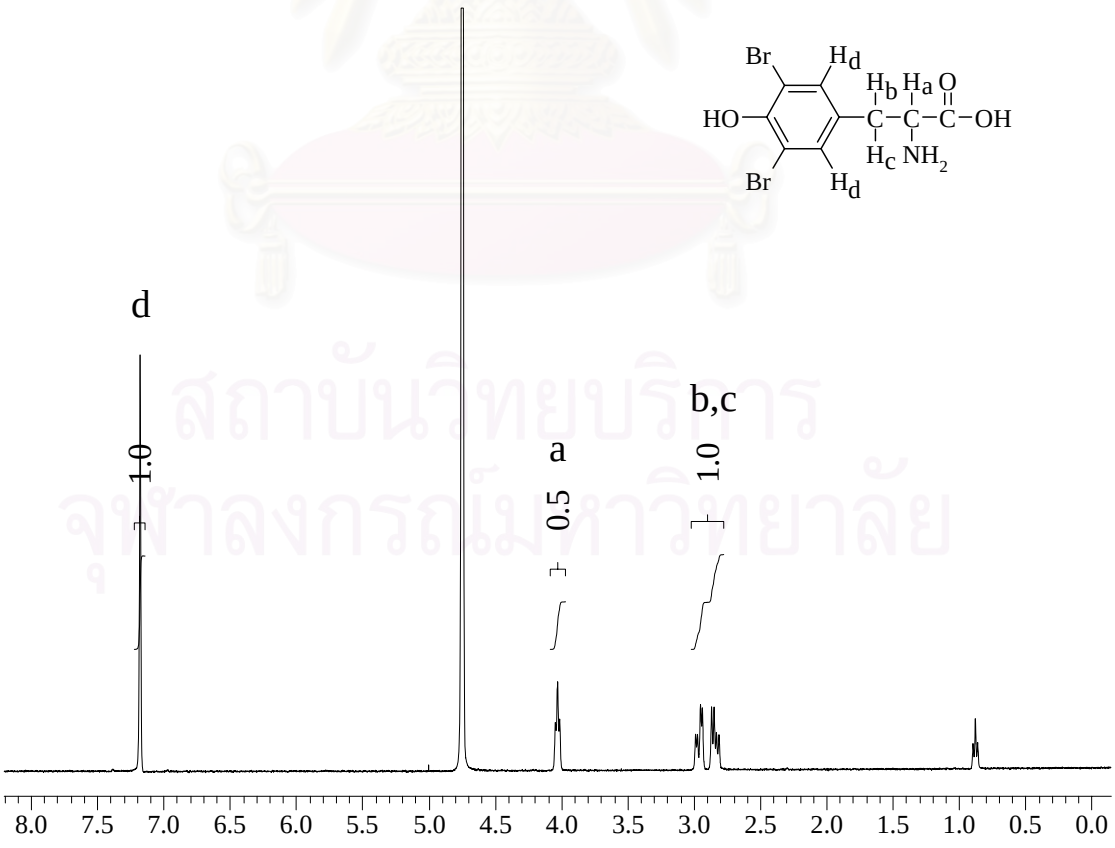

Figure 4.8 ^{1}H NMR spectrum of L-3,5-dibromotyrosine**.**

4.3.2 Attachment of L-3,5-Dibromotyrosine on the Surface of Activated Poly(DTE-*co*-20%DT carbonate) Film

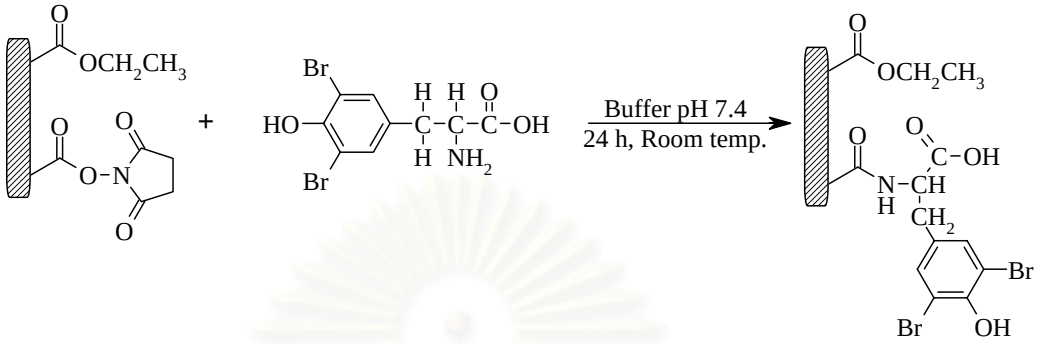

XPS was used to confirm the immobilization of L-3,5-dibromotyrosine on the activated poly(DTE-*co*-20%DT carbonate) surface. XPS data are outlined in Table 4.1. Theoretical atomic compositions calculated from atomic ratios of the chemical structures were also included for comparison. Controlled poly(DTE-*co*-20%DT carbonate) film is a virgin poly(DTE-*co*-20%DT carbonate) film that was exposed to the solution of L-3,5-dibromotyrosine simultaneously with the activated poly(DTE-*co*-20%DT carbonate) film. The fact that bromine composition was absent on the surface of controlled poly(DTE-*co*-20%DT carbonate) film indicated that the immobilization L-3,5-dibromotyrosine cannot take place without the activated succinimide group and there was no physisorption of L-3,5-dibromotyrosine on the surface. The atomic composition of the controlled film was quite consistent with the theoretical value. The theoretical percentage of bromine shown in the last row of the table was calculated based on the assumption that every single carboxyl group on the surface was converted to *N*-succinimide esters which later completely reacted with L-3,5-dibromotyrosine. %Substitution of L-3,5-dibromotyrosine on the surface calculated from XPS atomic composition was 92%. This outcome suggests that the activated carboxyl group in the form of *N*-succinimide ester was quite stable, yet reactive enough to interact with amino groups of the model peptide giving reasonably high % substitution. Such evidence also implies that the activated film should be able to react with RGD-containing peptides in a similar manner.

Table 4.1 Atomic composition of controlled poly(DTE-*co*-20%DT carbonate) film and NHS-activated poly(DTE-*co*-20%DT carbonate) film after L-3,5-dibromotyrosine attachment

Sample	Source	Atomic composition (%)			
		C	O	N	Br
Controlled poly(DTE-*co*-20%DT carbonate) film	XPS	71.4	24.2	4.4	-
	Theoretical	74.7	21.7	3.6	-
NHS-activated poly(DTE-*co*-20%DT carbonate) film after L-3,5-dibromotyrosine attachment	XPS	68.7	26.4	3.7	1.2
	Theoretical	73.5	21.2	4.0	1.3

4.4 Attachment of RGD-containing Peptides on the Surface of Activated Poly(DTE-*co*-20%DT carbonate) Film

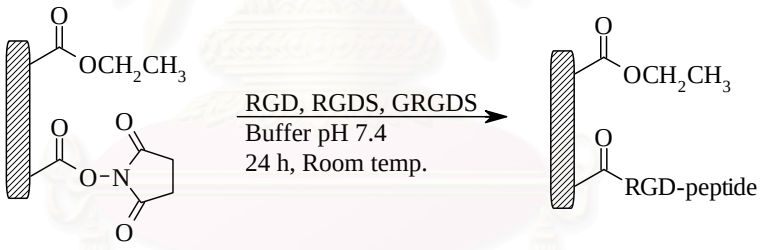

Three RGD-containing peptides: RGD, RGDS, GRGDS were chosen for this study. Their structures are shown in Figure 4.9.

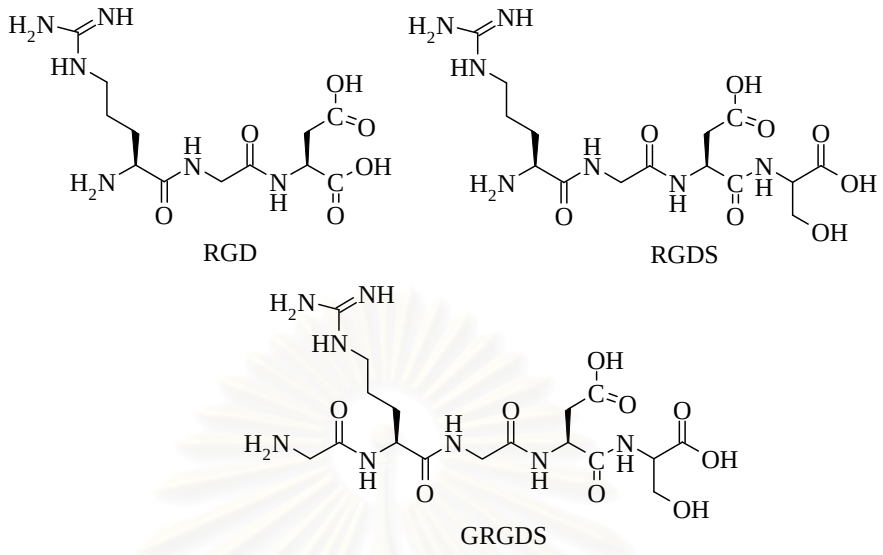

Figure 4.9 Chemical structures of RGD, RGDS and GRGDS

The amino group which is a part of peptide immobilized on the poly(DTE-*co*-20%DT carbonate) surface was quantified by ninhydrin method. The blue color which is a product of ninhydrin reacted with free amino groups (NH_2) has a maximum absorbance at 538 nm in 1,4-dioxane/2-propanol (1:1). Using 1,6-hexanediamine as a standard, a calibration curve was generated as shown in Figure 4.10.

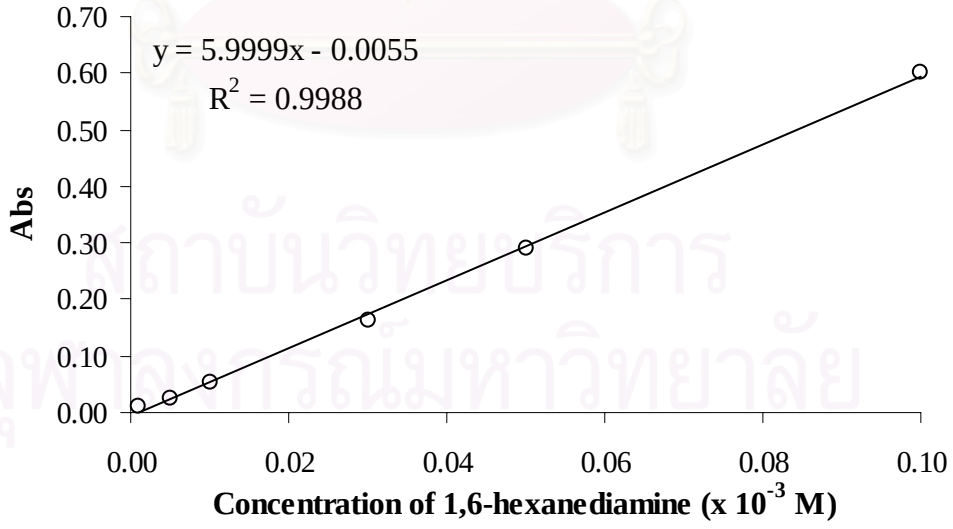

Figure 4.10 Calibration curve of UV absorbance as a function of 1,6-hexanediamine concentration using ninhydrin method.

4.4.1 Effect of Immobilization Time

Effect of reaction time on the immobilization of RGD on the surface of poly(DTE-*co*-20%DT carbonate) was determined by varying the reaction time from 2 to 48 h using the peptide concentration of 0.05 M. As displayed in Figure 4.11, the amino concentration per surface area was linearly increased as a function of reaction time within 24h and seemed to level off afterwards.

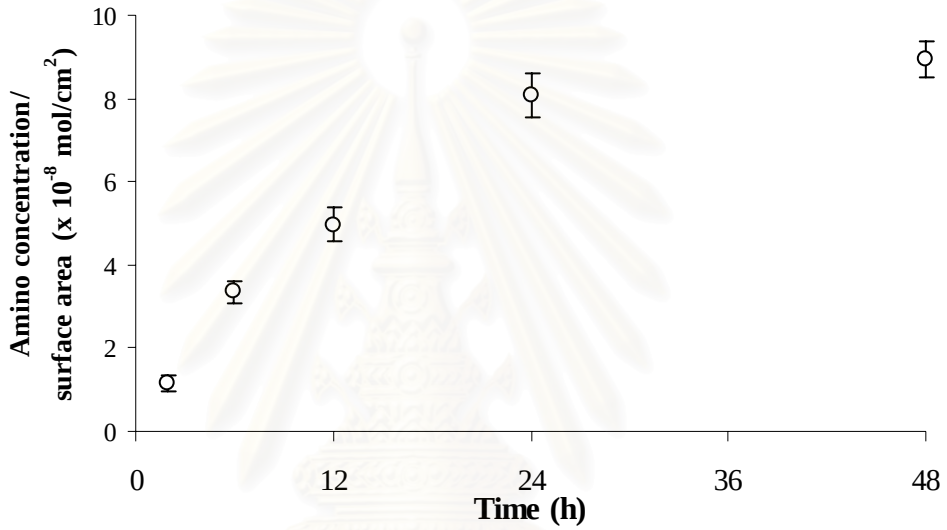

Figure 4.11 Amino concentration per surface area of immobilized RGD on poly(DTE-*co*-20%DT carbonate) surface as a function of immobilization time**.**

4.4.2 Effect of RGD-containing Peptide Concentration

The density of RGD-containing peptide or amino concentration/surface area on poly(DTE-*co*-20%DT carbonate) film was also influenced by RGD concentration. The data are illustrated in Figure 4.12. As the higher peptide concentration was used, the greater extent of peptide immobilization on the surface of poly(DTE-*co*-20%DT carbonate) was obtained. The density of immobilized RGD peptide of 16.1 x 10^{-8} mol/cm^2 was achieved after carrying the reaction using the RGD concentration of 0.05 M for 24 h.

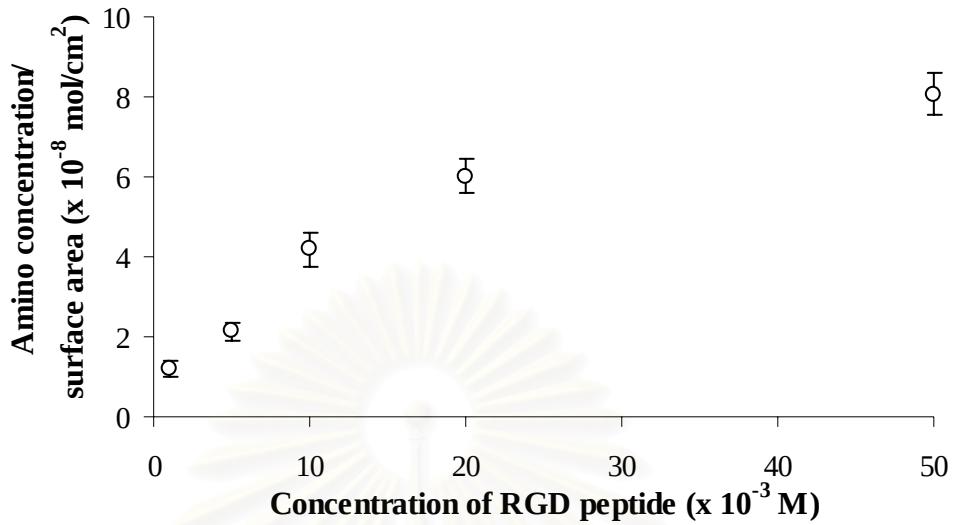

Figure 4.12 Amino concentration per surface area of immobilized RGD on poly(DTE-*co*-20%DT carbonate) surface as a function of peptide concentration**.**

4.4.3 Effect of RGD-containing Peptide

Using the concentration of peptide of 0.05 M and immobilization time of 24h, the extent of grafting of three RGD-containing peptides on the surface of activated poly(DTE-*co*-20%DT carbonate) were compared. As displayed in Figure 4.13, it seems that the longer peptide sequence, the lower the density of immobilized peptide. This trend may be explained by two reasons: (1) the bulkier structure of GRGDS in comparison with RGD and RGDS may lead to its lower reactivity to interact with the activated surface, (2) the limited solubility of the larger peptide in aqueous solution may account for the lower graft density of the immobilized GRGDS in comparison with other two sequences.

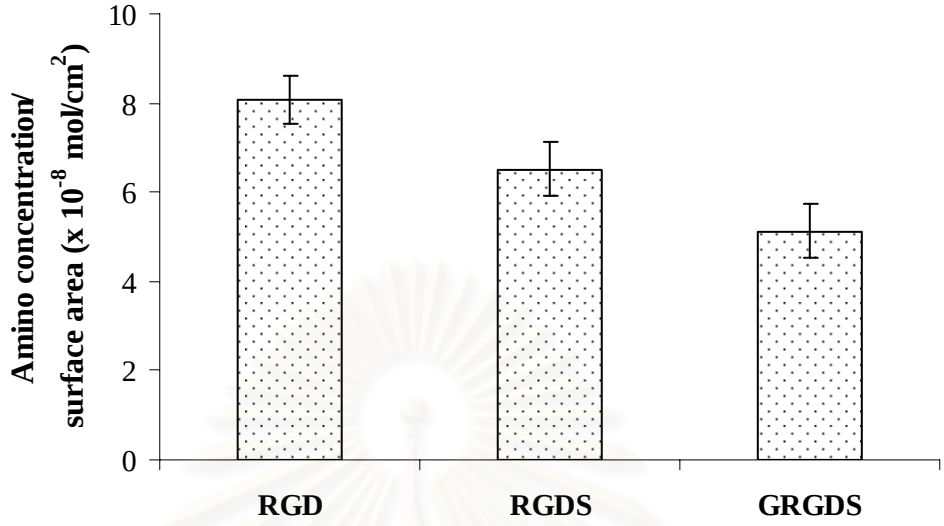

Figure 4.13 Amino concentration per surface area of immobilized RGD-containing peptides on poly(DTE-*co*-20%DT carbonate) surface using the peptide concentration of 0.05 M and immobilization time of 24h.

According to the ninhydrin analysis, the amino concentration per surface area which corresponds to the density of immobilized RGD-containing peptide is in the order of 10^{-8} mol/cm^2 in all cases. Such value is in fact much higher than 1 x 10^{-12} mol/cm^2 previously reported as a sufficient value that can promote the adhesion and spreading of fibroblast cells [25].

Since ninhydrin method is not a surface characterization technique, the calculated density of immobilized peptide may not reflect the actual density of immobilized peptide on the polymer surface. Therefore, XPS was additionally used to confirm the existence of RGD-containing peptide on the polymer surface. Taking into account that the virgin poly(DTE-*co*-20%DT carbonate) film, the activated poly(DTE-*co*-20%DT carbonate) films both before and after immobilization with RGD-containing peptide consist of the same basic elements (C, O, N), it is not possible to distinguish them by direct XPS analysis. In order to determine the success of peptide immobilization on the surface of the activated film, it is necessary to introduce a tag element that is different from those basic elements to the film after peptide immobilization before XPS analysis. Treating the film immobilized with RGD-containing peptide with heptafluorobutyryl chloride (HFBC) was chosen as a

route to introduce fluorine as a tag element. Heptafluorobutyryl chloride should be able to react with hydroxyl group which is a part of serine (S), an amino acid sequence at the end of GRGDS and RGDS.

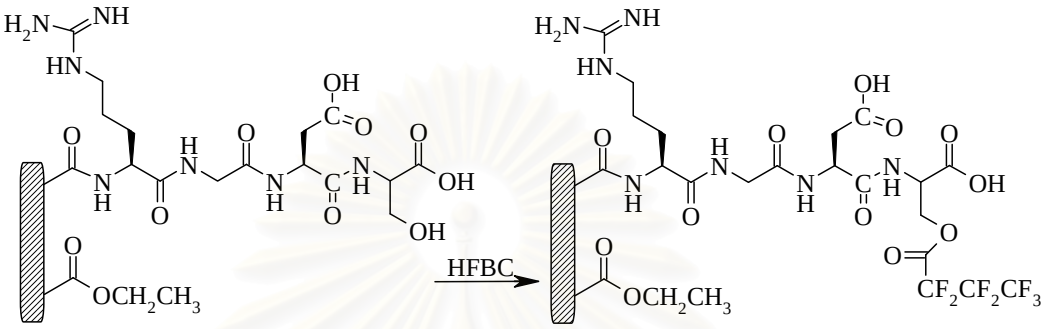

RGDS-poly(DTE-co-20%DT carbonate) film

HFBC = 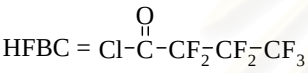

Atomic compositions of poly(DTE-*co*-20%DT carbonate) films immobilized with RGD-containing peptides are tabulated in Table 4.2. Percentages of fluorine follow the same trend that was previously observed from ninhydrin analysis. GRGDS, the longer peptide sequence, tended to give lower density than RGDS. The theoretical percentages of fluorine were calculated based on the assumption that every single carboxyl groups on the surface was converted to *N*-succinimide esters which later completely reacted with the RGD-containing peptides. Percentages of substitution of RGDS and GRGDS on the surface calculated from XPS atomic composition were 75% and 30%, respectively. As expected, there was no signal of fluorine detected on the surface of poly(DTE-*co*-20%DT carbonate) film immobilized with RGD because there are no reactive sites on either the polymer or the peptide that can react with heptafluorobutyryl chloride. However, assuming that RGD is more reactive than RGDS, its %substitution should be more than or at least equal to 75%.

Table 4.2 Atomic composition RGD-immobilized poly(DTE-*co*-20%DT carbonate) film after labeling with heptafluorobutyryl chloride

Sample	Source	Atomic composition (%)			
		C	O	N	F
RGD-poly(DTE-*co*-20%DT carbonate) film	XPS	69.1	25.0	5.4	-
	Theoretical	71.5	21.7	6.8	-
RGDS-poly(DTE-*co*-20%DT carbonate) film	XPS	68.9	4.5	23.7	2.9
	Theoretical	68.2	6.7	21.2	3.9
GRGDS- poly(DTE-*co*-20%DT carbonate) film	XPS	67.6	26.9	4.4	1.1
	Theoretical	67.8	21.3	7.1	3.8

4.5 Cell Study

In vitro cytocompatibility can be used as a primary indication of how cells response to a surface of interest. It is usually expressed in terms of cell adhesion and proliferation. Fibroblast cell line (B95) was used for this investigation. The cell adhesion ratio (CAR) is shown in Figure 4.14. The value of CAR is reported as a number of cells attached to a surface in proportion to a number of cells attached to tissue culture polystyrene (TCPS) in the same culture media. Having CAR value of 92%, virgin poly(DTE-*co*-20%DT carbonate) can be considered as a good substrate for cell adhesion as compared to 100% of TCPS. Evidently, the alteration of surface functionality has a significant impact on fibroblast adhesion and proliferation. Hydrophobic *N*-succinimide groups deteriorated the ability of the substrate to adhere cells. Adding soluble RGD (RGD-s) slightly increased the cell adhesion ratio of the virgin polymer film. The CAR values of RGD- and RGDS-immobilized surfaces were lower than expected considering that at least 75% of carboxyl groups on the polymer surfaces were immobilized with RGD or RGDS. The CAR value of poly(DTE-*co*-20%DT carbonate) film was raised from 92.3% to 117.0% after GRGDS immobilization even though its surface substitution was only 30%. The extra glycine

spacer obviously introduces flexibility to the polymer surface and thus allows the RGD part to effectively mediate its specific response to the cells.

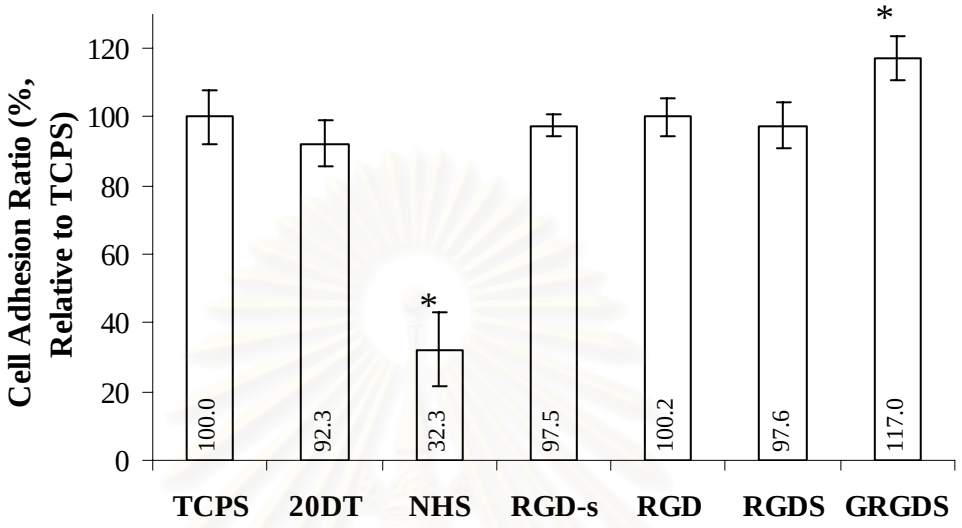

Figure 4.14 *In vitro* cell adhesion ratio (CAR) of fibroblasts on polymer substrates.
* This data are significantly different from other substrates ($p<0.01$).

According to cell proliferation ratio (CPR) shown in Figure 4.15, the RGD and RGDS-modified substrates became relatively poor substrates for cell proliferation unlike GRGDS-modified substrates. This set of data really confirmed that GRGDS can best enhance cytocompatibility of the polymer surface.

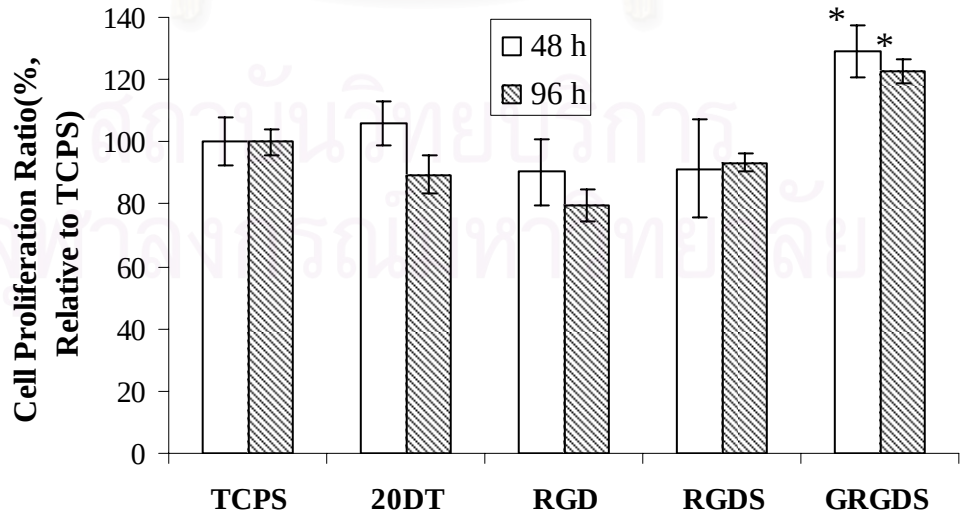

Figure 4.15 *In vitro* cell proliferation ratio (CPR) of fibroblasts on polymer substrates.
* This data are significantly different from other substrates ($p<0.01$).

CHAPTER V

CONCLUSION AND SUGGESTION

Immobilization of RGD-containing peptides on the surface of poly(DTE-*co*-20%DT carbonate) was successfully accomplished through a two-step reaction. The first step involved an activation of carboxyl groups by *N*-hydroxysuccinimide (NHS) in the presence of 1-(3-dimethylaminopropyl)-3-ethylcarbodiimide hydrochloride (EDCI). The activation of the poly(DTE-*co*-20%DT carbonate) surface with NHS was characterized by proton nuclear magnetic resonance (^{1}H-NMR) spectroscopy. An approximated bulk yield of 20% was obtained using the EDCI/NHS concentration of 0.1 M and a reaction time of 24 h in ethanol.

Reaction with L-3,5-dibromotyrosine, a model peptide, has demonstrated that the activated carboxyl group in the form of *N*-succinimide ester was quite stable, yet reactive enough to interact with amino groups of the model peptide giving reasonably high % substitution (~92%) The success of peptide immobilization in the second step was determined by X-ray photoelectron spectroscopy (XPS) and ninhydrin method. Using 1,6-hexamethylenediamine as a standard, the graft density of ~ 8.07 x 10^{-8}, 6.51 x 10^{-8}, and 5.13 x 10^{-8} mol/cm^2 was estimated for immobilization with RGD, RGDS, and GRGDS, respectively. According to XPS analysis of RGD-immobilized poly(DTE-*co*-20%DT carbonate) surface after labeling with heptafluorobutyryl chloride, 30 and 75 % substitution were calculated for immobilization with RGDS and GRGDS, respectively.

Results from *in vitro* cell studies suggested that the alteration of surface functionality has a significant impact on fibroblast (B95) adhesion and proliferation. Among all studied RGD-containing peptides, GRGDS can best enhance cytocompatibility of the polymer surface. Taking 100% of TCPS as a positive control, cell adhesion and proliferation ratios were elevated from 92.3 and 89.6% of the virgin polymer to 117.0 and 122.6% respectively, after GRGDS immobilization. The extra

glycine spacer presumably introduces the flexibility to the peptide and thus allows the RGD part to effectively mediate its specific response to the cells. This success would expand the applicability of this polymer in biomedical applications especially those requiring specific cellular response.

For future studies, attachment of other peptide sequences to improve specific cellular responses of poly(DTE-*co*-20%DT carbonate) surfaces are desirable. RGD-containing cyclic peptides are considered as potential candidates for improving cellular responses since their suitable conformation allows the RGD sequence to efficiently mediate its specific response to cells.

REFERENCES

1. Bourke, S. L., Kohn, J. Polymers derived from the amino acid L-tyrosine:polycarbonates, polyarylates and copolymers with poly(ethylene glycol) Advanced Drug Delivery Reviews 55 (2003): 447-466.

2. Kohn, J., Langer, R. Polymerization reactions involving the side chains of α-L-amino acids J. Am. Chem. Soc. 109 (1987): 817-820.

3. Pulapura, S., Kohn, J. Tyrosine derived polycarbonates: backbone modified, 'pseudo'-poly(amino acids)designed for biomedical applications Biopolymers 32 (1992): 411-417.

4. Tangpasuthadol, V., Pendharkar, S. M., Peterson, R. C. Kohn, J. Hydrolytic degradation of tyrosine-derived polycarbonates, a class of new biomaterials. Part I: study of model compounds Biomaterials 21 (2000): 2371-2378.

5. Tangpasuthadol, V., Pendharkar, S. M., Peterson, R. C. Kohn, J. Hydrolytic degradation of tyrosine-derived polycarbonates, a class of new biomaterials. Part II: 3-yr study of polymeric devices Biomaterials 21 (2000): 2379-2387.

6. Yu, C.; Kohn, J. Tyrosine-PEG-derived poly(ether carbonate)s as new biomaterials Part I: synthesis and evaluation Biomaterials 20 (1999): 253-264.

7. Pierschbacher, M.D., Ruoslahti, E. Cell attachment activity of fibronectin can be duplicated by small synthetic fragments of the molecule Nature 309 (1984): 30-33.

8. Ruoslahti, E., Pierschbacher, M. D. New perspectives in cell adhesion: RGD and integrins Science 238 (1987): 491-497.

9. Xiao, S. J. Tailored organic thin films on gold and titanium: peptide-grafting, protein resistance and physical characterization (Doctoral dissertation, Department of Materials, Swiss Federal Institute of Science and Technology Zürich, 1999)

10. Craig, W. S., Cheng, S., Mullen, D. G., Blevitt, J., Pierschbacher, M. D. Concept and progress in the development of RGD-containing peptide pharmaceuticals Biopolymers 37 (1995): 157-175.

11. Hersel, U., Dahmen, C., Kessler, H. RGD modified polymers: biomaterials for stimulated cell adhesion and beyond Biomaterials 24 (2003): 4385-4415.

12. Quirk, R. A., Chan, W. C., Davies M. C., Tendler, S. J. B., Shakesheff, K. M. Poly(L-lysine)-GRGDS as a biomimetic surface modifier for poly(lactic acid) Biomaterials 22 (2001): 865-872.

13. Jo, S.; Engel, P. S.; Mikos, A. G. Synthesis of poly(ethylene glycol)-tethered poly(propylene fumarate) and its modification with GRGD peptide Polymer 41 (2000): 7595-7604.

14. Morpurgo, M., Bayer, E. A., Wilchek, M. N-hydroxysuccinimide carbonates and carbamates are useful reactive reagents for coupling ligands to lysines on proteins J. Biochem. Biophys. Methods. 38 (1999): 17-28.

15. Marchand-Brynaert, J., Detrait, E., Noiset, O.; Boxus, T., Schneider, Y. J., Remacle, C. Biological evaluation of RGD peptidomimetics, designed for the covalent derivatization of cell culture substrata, as potential promotors of cellular adhesion Biomaterials 20 (1999): 1773-1782.

16. Xiao, S. J., Textor, M., Spencer, N. D. Covalent attachment of cell-adhesive, (Arg-Gly-Asp)-containing peptides to titanium surfaces Langmuir 14 (1998): 5507-5516.

17. Davis, D. H., Giannoulis, C. S., Johnson, R. W., Desai, T. A. Immobilization of RGD to <111> silicon surfaces for enhanced cell adhesion and proliferation Biomaterials 23 (2002): 4019-4027.

18. Yoon, J. J., Songa, S. H., Leeb, D. S., Park, T. G. Immobilization of cell adhesive RGD peptide onto the surface of highly porous biodegradable polymer scaffolds fabricated by a gas foaming/salt leaching method Biomaterials 25 (2004): 5613-5620.

19. Neff, J. A., Tresco, P. A., Caldwell, K. D. Surface modification for controlled studies of cell–ligand interactions Biomaterials 20 (1999): 2377-2993.

20. Marchand-Brynaert, J., Detrait, E.; Noiset, O., Boxus, T., Schneider, Y. J., Remacle, C. Biological evaluation of RGD peptidomimetics, designed for the covalent derivatization of cell culture substrata, as potential promotors of cellular adhesion Biomaterials 20 (1999): 1773-1782.

21. Neff, J. A., Tresco, P. A., Caldwell, K. D. A novel method for surface modification to promote cell attachment to hydrophobic substrates J. Biomed. Mater. Res. 40 (1998): 511-519.

22. Banerjee, P., Irvine, D.J., Mayes, A. M., Griffith, L. G. Polymer latexes for cell-resistant and cell-interactive surface J. Biomed. Mater. Res. 50 (2000): 331-339.

23. Alberts, B., Bray, J. L., Raff, M.; Roberts, K., Watson, J. D. Molecular biology of the cell. 3rd ed. New York: Garland Publishing, 1994.

24. Karp, G. Cell and molecular biology: concepts and experiments. 3rd ed. New York: John Wiley & Sons, 2002.

25. Ho, M. H., Wang, D. M., Hsieh, H. J., Liu, H. C., Hsien, T. Y., Lai, J. Y., Hou, L. T. Preparation and characterization of RGD-immobilized chitosan scaffolds Biomaterials 26 (2005): 3197-3206.

26. Mccaldin, D. J. The chemistry of ninhydrin Chemical Reviews 60 (1960): 39-51.

27. Wang, N. S. Amino acid assay by ninhydrin colorimetric method [online]. Available from: http://www.glue.umd.edu/~nsw/ench485/lab3a.htm [2004, February 1]

APPENDICES

APPENDIX A

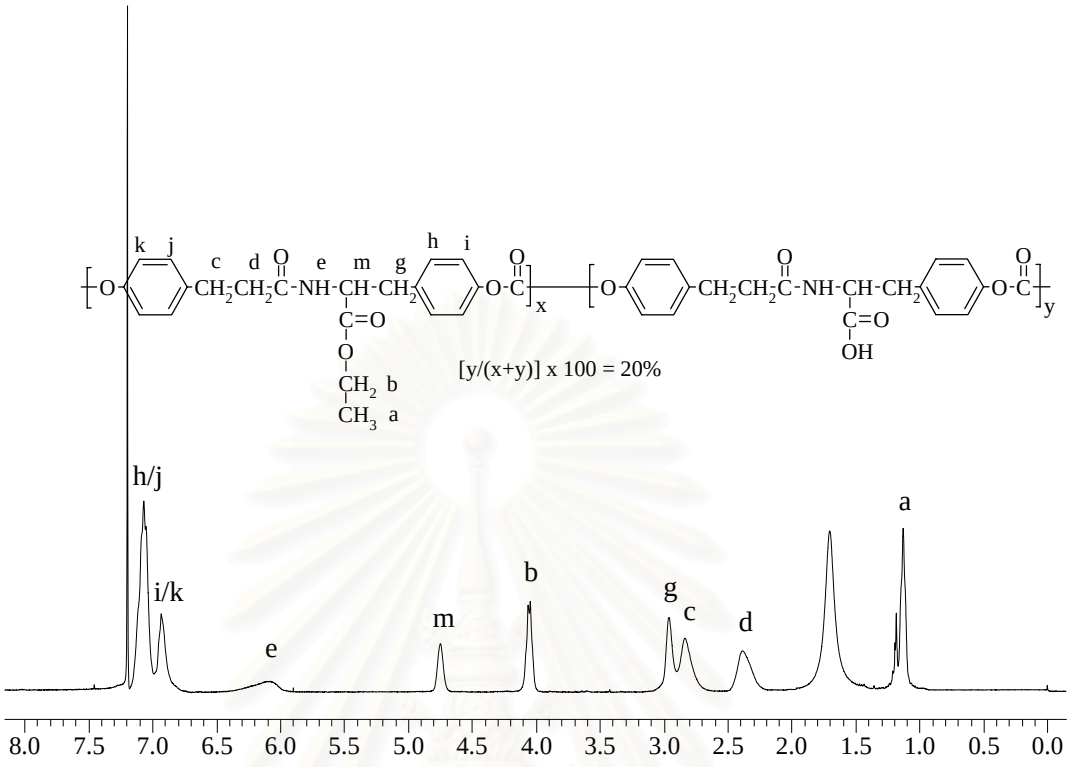

Figure A-1 The ^{1}H-NMR (400 MHz $CDCl_3$) of poly(DTE-*co*-20%DT carbonate) film

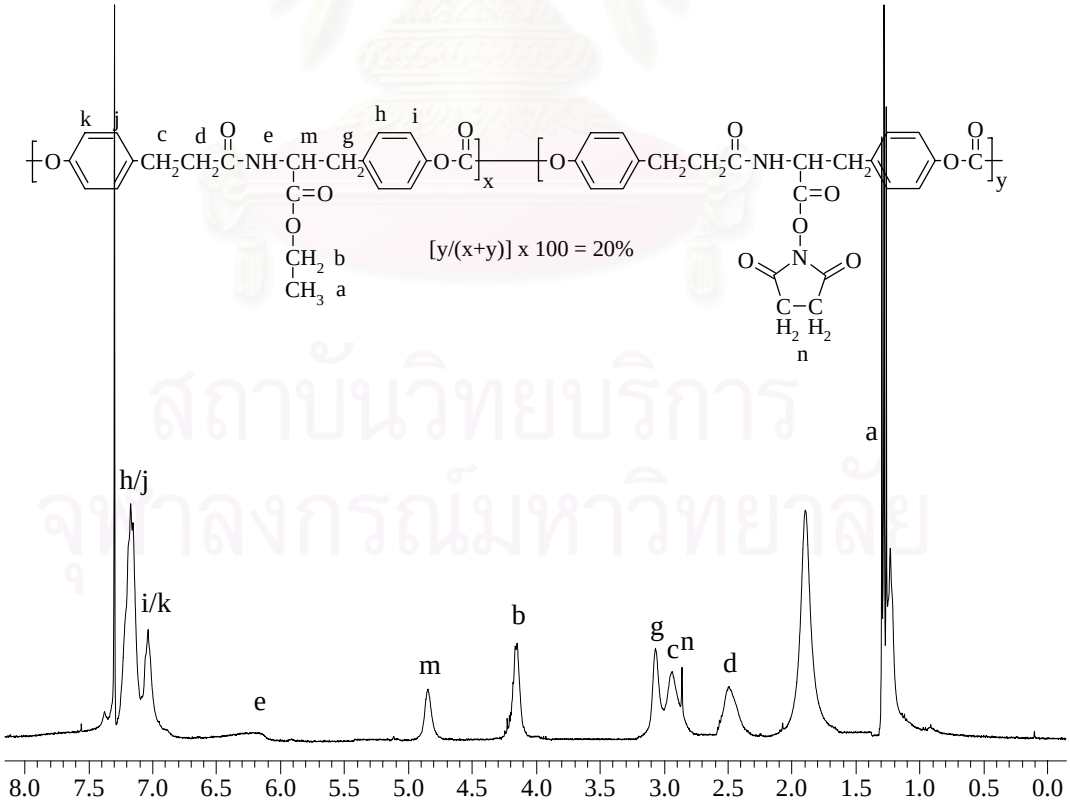

Figure A-2 The ^{1}H-NMR (400 MHz $CDCl_3$) of activated poly(DTE-*co*-20%DT carbonate) film

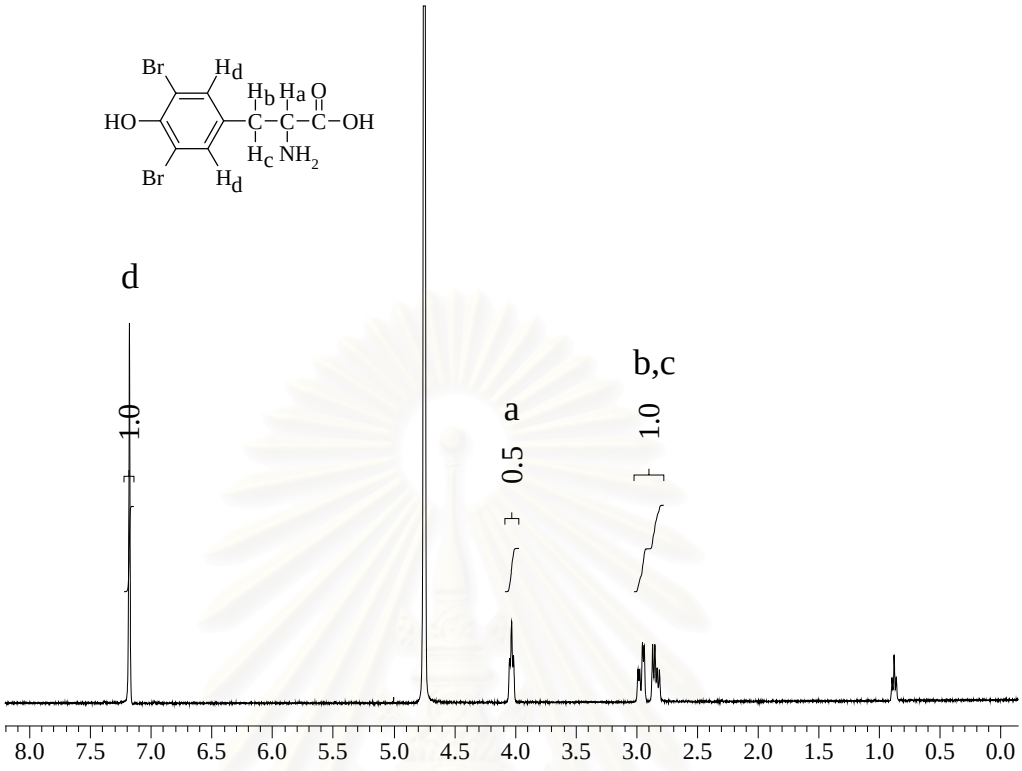

Figure A-3 The ^{1}H-NMR (400 MHz DCl) of L-3,5-dibromotyrosine

APPENDIX B

Table B-1 Water contact angle of activated poly(DTE-*co*-20%DT carbonate) films after reaction with *N*-hydroxysuccinimide in water as a function of reaction time.

Time (min)	Advancing water contact angle (θ_A) (degree)	Receding water contact angle (θ_R) (degree)
0	71.5 ± 0.77	29.8 ± 1.12
30	75.5 ± 1.18	27.0 ± 1.67
60	76.3 ± 1.79	25.9 ± 1.04
90	77.5 ± 1.28	34.0 ± 1.55
120	81.7 ± 0.90	32.6 ± 1.58
150	83.6 ± 0.49	38.6 ± 1.48
180	84.0 ± 0.77	37.8 ± 1.79
210	83.4 ± 0.92	39.0 ± 1.41
240	84.6 ± 0.92	36.1 ± 1.58

The advancing contact angles of all activated poly(DTE-*co*-20%DT carbonate) films were significantly higher than that of poly(DTE-*co*-20%DT carbonate) film ($p<0.01$).

Table B-2 %Yield of activation of poly(DTE-*co*-20%DT carbonate) with *N*-hydroxysuccinimide as a function of coupling agent concentration.

Concentration of coupling agent (M)		% yield
[EDCI]	[NHS]	
0.01	0.01	0.5
0.02	0.02	1.6
0.03	0.03	2.0
0.04	0.04	4.5
0.05	0.05	6.6
0.06	0.06	9.4
0.07	0.07	11.8
0.10	0.10	19.8

Table B-3 %Yield of activation of poly(DTE-*co*-20%DT carbonate) with *N*-hydroxysuccinimide as a function of reaction time.

Time (h)	% Yield	
	[EDCI] = [NHS] = 0.05 M	[EDCI] = [NHS] = 0.10 M
0.5	3.9	7.9
1	5.7	13.8
2	6.6	19.8
3	6.2	20.1
4	7.0	21.0

Determination of Amino Groups of Modified poly(DTE-*co*-20%DT carbonate) Films

Table B-4 UV-absorbance at λ = 538 nm of standard 1,6-hexanediamine solution for generating a calibration curve

Concentration of 1,6-hexanediamine ($\times 10^{-3}$ M)	Abs
0.001	0.012
0.005	0.025
0.010	0.052
0.030	0.164
0.050	0.290
0.100	0.600

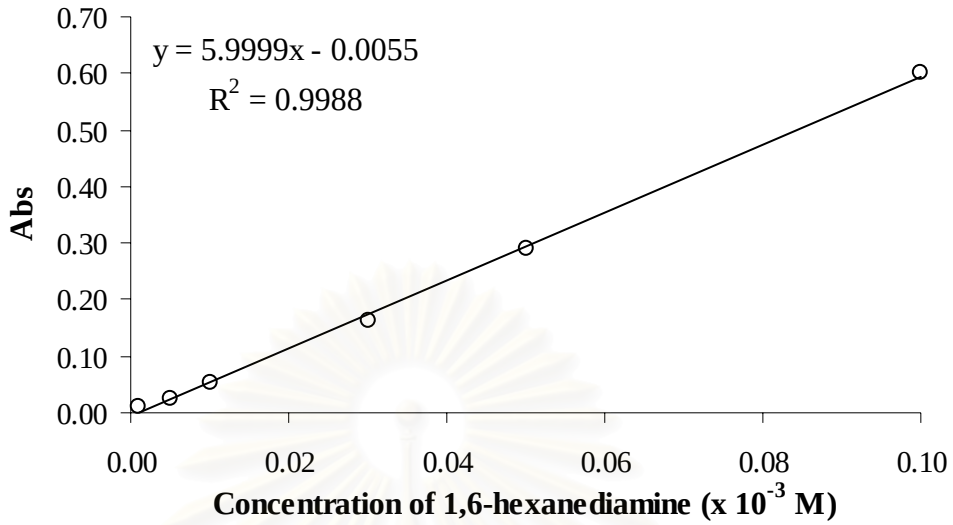

Figure B-1 Calibration curve of UV-absorbance as a function of 1,6-hexanediamine concentration analyzed by ninhydrin method.

Table B-5 Amino content of RGD-poly(DTE-*co*-20%DT carbonate) film as a function of immobilization time.

Time (h)	Abs	Concentration (x 10^{-8} mole/cm^2)	Average ± S.D. (x 10^{-8} mole/cm^2)
2	0.028	0.99	1.16 ± 0.20
	0.034	1.16	
	0.045	1.49	
	0.032	1.11	
	0.030	1.05	
6	0.110	3.40	3.35 ± 0.27
	0.099	3.08	
	0.118	3.64	
	0.115	3.55	
	0.098	3.05	
12	0.180	5.47	4.97 ± 0.39
	0.152	4.64	
	0.175	5.32	
	0.153	4.67	
	0.155	4.73	
24	0.287	8.62	8.07 ± 0.53
	0.245	7.38	
	0.264	7.94	
	0.286	8.59	
	0.260	7.83	
48	0.275	8.27	8.96 ± 0.43
	0.311	9.33	
	0.295	8.86	
	0.310	9.30	
	0.302	9.06	

The amino contents of all RGD- immobilized poly(DTE-*co*-20%DT carbonate) films were significantly higher ($p<0.01$) than that of poly(DTE-*co*-20%DT carbonate) film.

Table B-6 Amino content of RGD-poly(DTE-*co*-20%DT carbonate) film as a function of RGD concentration.

Concentration of RGD peptide (x 10^{-3} M)	Abs	Concentration (x 10^{-8} mole/cm^2)	Average ± S.D. (x 10^{-8} mole/cm^2)
1	0.042	1.40	1.20 ± 0.21
	0.040	1.34	
	0.037	1.25	
	0.034	1.16	
	0.024	0.87	
5	0.077	2.43	2.14 ± 0.22
	0.059	1.90	
	0.073	2.31	
	0.062	1.99	
	0.065	2.08	
10	0.141	4.32	4.17 ± 0.42
	0.138	4.23	
	0.122	3.76	
	0.123	3.79	
	0.157	4.79	
20	0.211	6.38	6.02 ± 0.43
	0.204	6.17	
	0.195	5.91	
	0.175	5.32	
	0.209	6.62	
50	0.287	8.62	8.07 ± 0.53
	0.245	7.38	
	0.264	7.94	
	0.286	8.59	
	0.260	7.83	

The amino contents of all RGD- immobilized poly(DTE-*co*-20%DT carbonate) films were significantly higher ($p<0.01$) than that of poly(DTE-*co*-20%DT carbonate) film.

Table B-7 Amino content of RGDS-poly(DTE-*co*-20%DT carbonate) and GRGDS-poly(DTE-*co*-20%DT carbonate) using peptide concentration of 0.05 M.

RGD-peptide	Abs	Concentration (x 10^{-8} mole /cm^2)	Average ± S.D. (x 10^{-8} mole/cm^2)
RGDS	0.222	6.71	6.51 ± 0.61
	0.216	6.53	
	0.199	6.03	
	0.194	5.88	
	0.246	7.41	
GRGDS	0.180	5.47	5.13 ± 0.60
	0.134	4.11	
	0.177	5.38	
	0.167	5.08	
	0.185	5.61	

The amino content of RGD-immobilized poly(DTE-*co*-20%DT carbonate) films was significantly higher ($p<0.01$) than those of the RGDS-immobilized poly(DTE-*co*-20%DT carbonate) film and GRGDS-immobilized poly(DTE-*co*-20%DT carbonate) film. There was significant ($p<0.05$) difference between the amino content of RGDS-immobilized poly(DTE-*co*-20%DT carbonate) film and that of GRGDS-immobilized poly(DTE-*co*-20%DT carbonate) film.

Table B-8 Number of fibroblast attachment on polymer surface after 12 h incubation.

Polymer surface	Number of fibroblast attachment (cells/cm^3)	% CAR
poly(DTE-*co*-20%DT carbonate)	2283 ± 155	92.3 ± 6.78
NHS-poly(DTE-*co*-20%DT carbonate)	799 ± 86	32.3 ± 10.80
RGD-poly(DTE-*co*-20%DT carbonate)	2479 ± 136	100.2 ± 5.48
soluble RGD + poly(DTE-co-20%DT carbonate)	2412 ± 79	97.5 ± 3.26
RGDS-poly(DTE-*co*-20%DT carbonate)	2416 ± 158	97.6 ± 6.56
GRGDS-poly(DTE-*co*-20%DT carbonate)	2896 ± 183	117.0 ± 6.31
Tissue culture polystyrene (TCPS)	2475 ± 196	100.0 ± 7.91

The number of fibroblasts attached on GRGDS-immobilized poly(DTE-*co*-20%DT carbonate) films was significantly higher ($p<0.01$) than those of the poly(DTE-*co*-20%DT carbonate) film, RGD-immobilized poly(DTE-*co*-20%DT carbonate) film, RGDS-immobilized poly(DTE-*co*-20%DT carbonate) film, soluble RGD + poly(DTE-*co*-20%DT carbonate) and TCPS. There are no significant difference of the number of fibroblast attachment among TCPS, poly(DTE-*co*-20%DT carbonate), RGD-poly(DTE-*co*-20%DT carbonate), RGDS-poly(DTE-*co*-20%DT carbonate) and soluble RGD + poly(DTE-*co*-20%DT carbonate) ($p > 0.05$).

Table B-9 Number of fibroblast proliferation on polymer surface

Polymer surface	48 h proliferation		96 h proliferation	
	Cell Number (x100 cells/cm^3)	% CPR	Cell Number (x 100 cells/cm^3)	% CPR
poly(DTE-*co*-20%DT carbonate)	193 ± 14	106.0 ± 7.2	642 ± 41	89.6 ± 6.3
RGD-poly(DTE-*co*-20%DT carbonate)	164 ± 17	90.3 ± 10.5	569 ± 29	79.4 ± 5.1
RGDS-poly(DTE-*co*-20%DT carbonate)	166 ± 26	91.3 ± 17.5	670 ± 21	93.4 ± 3.1
GRGDS-poly(DTE-*co*-20%DT carbonate)	236 ± 20	129.3 ± 8.3	879 ± 32	122.6 ± 3.6
Tissue culture polystyrene (TCPS)	182 ± 14	100.0 ± 7.7	717 ± 30	100 ± 4.0

The number of fibroblast proliferation on GRGDS-immobilized poly(DTE-*co*-20%DT carbonate) films was significantly higher ($p<0.01$) than those of the poly(DTE- *co*-20%DT carbonate) film, RGD-immobilized poly(DTE-*co*-20%DT carbonate) film, RGDS-immobilized poly(DTE-*co*-20%DT carbonate) film and TCPS.

APPENDIX C

Amino Acid Assay by Ninhydrin Colorimetric Method [26, 27]

The reaction between alpha-amino acid and ninhydrin involve the development of color which can be described by the following five mechanistic steps:

alpha-amino acid + ninhydrin ---> reduced ninhydrin + alpha-amino acid + H_2O (A-1)

alpha-amino acid + H_2O ---> alpha-keto acid + NH_3 (A-2)

alpha-keto acid + NH_3 ---> aldehyde + CO_2 (A- 3)

Step (A-1) is an oxidative deamination reaction that removes two hydrogens from the alpha-amino acid to yield an alpha-imino acid. Simultaneously, the original ninhydrin is reduced and loses an oxygen atom with the formation of a water molecule. In Step (A-2), the NH group in the alpha-amino acid is rapidly hydrolyzed to form an alpha-keto acid with the production of an ammonia molecule. This alpha-keto acid further undergoes decarboxylation reaction in Step (A-3) under heated condition to form an aldehyde that has one less carbon atom than the original amino acid. A carbon dioxide molecule is also produced. These first three steps produce the reduced ninhydrin and ammonia that are required for the production of blue color. The overall reaction for the above reactions is simply expressed in equation (A-4) as follows:

alpha-amino acid + 2 ninhydrin ---> CO_2 + aldehyde + final complex (blue) + $3H_2O$ (A-4)

In summary, ninhydrin, which is originally yellow, reacts with amino acid and turns into deep purple. It is this purple color that is detected in this method. Ninhydrin will react with a free alpha-amino group of NH_2-CHR-COOH. This group is a part of all amino acids, peptides, or proteins. Whereas, the decarboxylation reaction would proceed for a free amino acid and a free amino group at chain end or side chain of

protein or peptide, it does not occur for an amino group within peptides and proteins. Thus, theoretically only amino acids will lead to the color development. However, one should always check out the possible interference from peptides and proteins by performing blank tests especially when such solutions are readily available. For example, one can simply add the ninhydrin reagent to a solution of only proteins and see if there is any color development. There is no excuse for failing to perform such a vital test when the sample mixture contains both proteins and amino acids. There are also reports that chemical compounds other than amino acids also yield positive results.

This test can be used routinely for the detection of glycine in the absence of other interfering species. Although this is a fast and sensitive test for the presence of alpha-amino acids because of the nonselectivity, it cannot be used to analyze the relative individual contents of a mixture of different amino acids. Furthermore, the color intensity developed is dependent on the type of amino acid. Finally, it does not react with tertiary or aromatic amines.